Review

Molecular Imaging with PET

Simon M. Ametamey, Michael Honer, and Pius August Schubiger

Chem. Rev., **2008**, 108 (5), 1501-1516 • DOI: 10.1021/cr0782426 • Publication Date (Web): 22 April 2008

Molecular Imaging with PET

Simon M. Ametamey,* Michael Honer, and Pius August Schubiger

Center for Radiopharmaceutical Science of ETH, PSI and USZ, Department of Chemistry and Applied Biosciences of ETH, CH-8093 Zurich, Switzerland

Received December 18, 2007

Contents

1. Introduction

1.1. Definition of Molecular Imaging

Recent advances in noninvasive imaging modalities have opened endless opportunities for molecular diagnostic and therapeutic procedures. The term "molecular imaging" is broadly used in conjunction with imaging modalities that provide anatomic as well as functional information. But is anatomic imaging really molecular imaging? And do imaging studies involving blood pool, perfusion, or skeleton provide us with molecular images? Clearly, the terminology "molecular imaging" is quite often used for marketing rather than for scientific purposes, as pointed out by Haberkorn and Eisenhut in an EJNM editorial.[1]

Literally speaking, molecular imaging can be interpreted as imaging using molecules or imaging of molecules. But if we consider that molecular imaging aims to target a specific tissue or cell type using a specific imaging probe, then certainly molecular imaging must be defined as the visualization of *in vivo* biological processes at the molecular or cellular level using specific imaging probes. This and similar definitions have been formulated in the literature by many authors[2–5] and most recently by the Molecular Imaging Center of Excellence Standard Definition Task Force.[6] In this latter definition, the techniques mentioned are radiotracer imaging/nuclear medicine, magnetic resonance (MR) imaging, MR spectroscopy, optical imaging, ultrasound, and others.

Molecular imaging may be used for early detection, characterization, and "real time" monitoring of disease as well as investigating the efficacy of drugs. Presently, there is a consensus among experts in the field that the most sensitive molecular imaging techniques are the radionuclide-based positron emission tomography (PET) and single photon emission computed tomography (SPECT) imaging modalities. PET or SPECT has the sensitivity needed to visualize most interactions between physiological targets and ligands such as neurotransmitters and brain receptors. Radionuclide-based imaging modalities are able to determine concentrations of specific biomolecules as low as in the picomolar range. It must be stressed here, however, that the choice of a certain imaging modality whether MRI, ultrasound, or PET depends primarily on the specific question to be addressed.

Over the years, biologically interesting molecular probes for PET imaging have been developed and used for diagnostic clinical studies, basic human studies for understanding biochemical processes in neurobiology, and preclinical studies especially using nonhuman primates and rodents. In recent years, the PET technology has been applied in various ways to assist in drug development, whereby understanding drug action, establishing dosage regimens of central nervous system (CNS) drugs, and treatment strategies have been most crucial. Such studies eventually provide means to accomplish "personalized medicine" by monitoring individual response to drug delivery.

Central to molecular imaging with PET is the development of appropriate PET imaging probes. Although the development of PET radiopharmaceuticals for the *in vivo* imaging of specific targets in the CNS began more than 25 years ago,

* Corresponding author. Tel.: +41 44 6337463. Fax: +41 44 6331367. E-mail: simon.ametamey@pharma.ethz.ch.

10.1021/cr0782426 CCC: $71.00
Published on Web 04/22/2008

Simon M. Ametamey received his M.S. in Chemistry at the Technical University of Merseburg, Germany, in 1985. He earned his doctorate degree in Organic Chemistry from University of Zurich, Switzerland, under the direction of Prof. H. H. Heimgartner. After a postdoctoral study with Prof. K. Bernhard (Hoffmann La Roche, Basel, Switzerland) he joined in 1991 the Center for Radiopharmaceutical Science of ETH, PSI and USZ in Villigen, Switzerland, and in 1995 became the group leader of the Radiotracer Synthesis research group. In 2006, he was appointed Titularprofessor and is currently cohead of the newly established Animal Imaging Center-PET at the Institute of Pharmaceutical Science at ETH. His current research interests are in the development of PET radiopharmaceuticals for diagnostic application in brain diseases and tumor imaging.

Michael Honer studied biochemistry at the University of Tübingen, Germany, and the Federal Institute of Technology (ETH) in Zürich, Switzerland, from where he received his M.S. degree in 1994. He pursued his Ph.D. in neuropharmacology with Professor Hanns Möhler at the Institute of Pharmacology of ETH and University Zürich. On completion of his Ph.D. in 1999, he moved to the Center of Radiopharmaceutical Science at the Paul Scherrer Institute (PSI) in Villigen, Switzerland, to carry out research on the pharmacological characterization of novel PET radioligands. In 2005, he became team leader at the newly established Animal Imaging Center (AIC) at the Institute of Pharmaceutical Science at ETH to work on small animal PET imaging. His current research interests include the standardization and refinement of experimental PET protocols as well as the quantifiability and reproducibility of small animal PET data.

until today only a handful of established PET radiopharmaceuticals exist for the imaging of some CNS targets. For a vast majority of CNS targets, there are currently no suitable PET radioligands. As with drug development, the difficulty in radioligand development is the fact that *in vivo* factors such as *in vivo* affinity, specific binding, metabolic stability, and pharmacokinetics are for the most part unknown. Quite often, initial lead compounds as potential imaging probes go through several steps of optimization before the imaging probe with the desirable imaging characteristics including selectivity and high specific binding is selected for imaging. Thus, many months may be required before the optimal PET molecular imaging probe gets through radiosynthesis and animal studies into clinical trials. Section 3 of this review provides a discussion on some of the most important criteria that are necessary for a successful CNS molecular probe.

Since October 1, 1997, P. August Schubiger has been full Professor of Radiopharmacy at the Institute of Pharmaceutical Sciences at the Swiss Federal Institute of Technology (ETH) Zurich. He heads the Center for Radiopharmaceutical Science of the ETH, the Paul Scherrer Institute (PSI), and at the Clinic and Polyclinic for Nuclear Medicine at the University of Zurich. Prof. Schubiger studied chemistry at the University of Zurich and got his Ph.D. in 1972. He followed one year postdoctoral work in radiochemistry at the Federal Institute for Reactor Physics, one year as an IAEA expert in Brazil, and two and a half years at the Max Planck Institute for Nuclear Physics in Heidelberg. In 1979, he took a position in the radiopharmacy division of the PSI, of which he has been the head since 1989. The main activities of the radiopharmacy research are the development of radioactively labeled molecules, which bind specifically to defined structures. Such functional radiopharmaceuticals can serve both as diagnostic agents in nuclear medicine and as therapeutic agents for use against tumor metastases.

Table 1. Physical Properties of Commonly Used Positron-Emitting Radionuclides

nuclide	half-life (min)	maximum energy (MeV)	mode of decay (%)	theoretical specific activity (GBq/μmol)
^{18}F	110	0.64	β+ (97%) EC[a] (3%)	6.3×10^4
^{11}C	20.3	0.97	β+ (99%)	3.4×10^5
^{13}N	10	1.20	β+ (100%)	7.0×10^5
^{15}O	2	1.74	β+ (100%)	3.4×10^6
^{76}Br	972	4.0	β+ (57%) EC (43%)	7.2×10^3
^{124}I	60 192	2.14	β+ (25%) EC (75%)	1.15×10^3
^{68}Ga	68.1	1.90	β+ (89%) EC (11%)	1.02×10^5
^{64}Cu	762	0.655	β+ (19%) EC (41%) β+ (40%)	9.13×10^3

[a] EC: electron capture.

Several PET nuclides exist for incorporation into biomolecules (Table 1), but most of the PET imaging probes applied in neurological research have been labeled with either ^{11}C or ^{18}F. We describe the radiolabeling strategies that are commonly employed for the synthesis of ^{11}C- and ^{18}F-labeled PET imaging probes. Furthermore, we give an overview of the most useful clinical PET radiopharmaceuticals that have found application for the CNS with emphasis on dopaminergic, serotonergic, cholinergic, and glutamatergic systems as well as beta-amyloid imaging agents for the diagnosis of Alzheimer's disease (AD). Small animal PET imaging has helped to establish PET as a leading tool in molecular

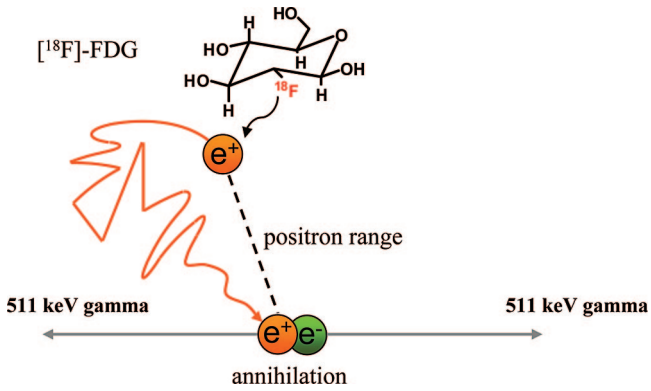

Figure 1. Principle of PET imaging. ^{18}F atom on the sugar molecule decays by emitting a positron, a positively charged electron.

imaging, making possible the translation of research results from bench to the bedside. We highlight also the challenges facing small animal PET imaging and some of its applications in rodent models of human brain diseases.

1.2. PET Methodology

PET imaging agents are radiolabeled with positron-emitting radionuclides, which decay by the emission of a positively charged particle, the positron. After being emitted from the nucleus the positron travels a short distance in the surrounding matter or tissue before it annihilates with an electron (Figure 1). The distance traveled by the positron before annihilation is known as positron range. The energies of the emitted positrons determine the path length before annihilation and are different for each positron-emitting radionuclide (Table 1). The larger the positron energy, the larger the average distance the positron travels before annihilating and the larger the loss in spatial resolution. Annihilation produces two 511 keV γ-rays, which correspond to the rest masses of the positron and electron. The two γ-rays are emitted simultaneously in opposite directions and are then detected by an array of surrounding detectors. A detector pair gives rise to a line along which positron annihilation must have occurred. Although the exact site of annihilation is unknown, the acquisition of a large number of coincidence events along all the lines can provide information to reconstruct the numerous events that have been registered into an image with information on the spatial distribution of radioactivity as a function of time (for a review see Levin).[7]

A special advantage of PET is that the measured tissue radioactivity can be measured in absolute units (Bq/mL); however, prior corrections for physical effects such as photon attenuation and random and scattered radiation must be made. Modern PET cameras collect data in either two- or three-dimensional modes.

1.3. Radionuclides for PET Imaging

Among the nuclear medicine imaging modalities, PET offers a specific advantage because it employs positron-emitting isotopes of atoms such as carbon, nitrogen, and oxygen, the main constituents of bioorganic molecules, and thus allows the syntheses of radiopharmaceuticals that are chemically indistinguishable from their nonradioactive counterparts. Apart from a negligible isotopic effect, the radiolabeled pharmaceutical possesses the same physicochemical and biochemical properties as the nonlabeled compound. Whereas the replacement of a carbon-12 or nitrogen-14 atom with carbon-11 or nitrogen-13 nuclide, respectively, is isotopic substitution, the radiolabeling with fluorine-18 is mainly nonisotopic substitution. Fluorine atom is generally not a constituent of biomolecules, but the substitution of a hydrogen atom or hydroxyl group by a fluorine atom is one of the most commonly applied bioisosteric replacements. Steric parameters for fluorine and hydrogen are similar (van der Waal's radii of fluorine and hydrogen are 1.35 and 1.20 Å, respectively), and the replacement of hydrogen for fluorine in a biomolecule induces only minimum steric perturbations.[8] The strong electron-withdrawing properties of fluorine, however, result in pharmaceuticals with altered electronic properties, lipophilicity, and biological characteristics. In some cases, the fluorinated compounds even exhibit improved potency when compared to the nonfluorinated analogues. For example, it was shown in a study with naphthyl-fused diazepines that aromatic substitution of a fluorine atom for a hydrogen atom resulted in enhanced affinity and efficacy.[9] With regard to lipophilicity, bioisosteric replacement of a hydrogen atom in an aliphatic position by fluorine will generally decrease the lipophilicity, while substitution in an aryl group increases the lipophilicity.[10]

Of all the positron emitters employed in PET, fluorine-18 labeled PET radiopharmaceuticals have the most favorable physical properties because the fluorine-18 nuclide has the best imaging physical characteristics due to the low positron energy (Table 1). Its optimal physical half-life of 110 min allows for more complex radiosynthesis, longer *in vivo* investigation, and, most importantly, "satellite" and commercial distribution to clinical PET centers that lack radiochemistry facilities. Prominent representative examples of fluorine-18 labeled PET imaging probes synthesized by nonisotopic substitution are 6-[^{18}F]-fluoro-3,4-dihydroxyphenylalanine ([^{18}F]6-Fluoro-L-DOPA), a PET ligand for probing cerebral dopamine metabolism[11,12] and neuroendocrine tumors in humans,[13] and 2-[^{18}F]-fluoro-deoxy-D-glucose ([^{18}F]FDG) (Figure 2), for studying glucose metabolism.[14] [^{18}F]FDG is the best clinically known and the most successful commercial PET radiopharmaceutical. All experts in the field agree that there would be no clinical PET imaging today without [^{18}F]FDG.

Carbon-11, a positron-emitting isotope of carbon with a physical half-life of 20.3 min, is particularly suited for labeling compounds with short biological half-lives. Compared to fluorine-18, the relatively short physical half-life of ^{11}C allows repeated investigations in the same subject and within short time intervals. A disadvantage, however, is the fact that carbon-11 labeled compounds can be produced and used only in centers with a cyclotron and radiochemistry facility.

In Table 1 are shown some commonly used PET nuclides including the "nonstandard" radionuclides and their physical properties. Except for gallium-68, which is a generator-produced PET nuclide, all other positron emitters shown in Table 1 are produced in a cyclotron by the bombardment of an appropriate target material with either accelerated protons or deuterons. Several other positron-emitting radionuclides such as ^{64}Cu, ^{76}Br, or ^{124}I, with half-lives longer than fluorine-18, are useful for studying biochemical processes with slow pharmacokinetics in addition to making satellite delivery much easier.

1. X = OH, D-Glucose
2. X = ^{18}F, 2-Fluoro-2-deoxy-D-glucose

3. X = H, 3,4-Dihydoxyphenylalanine (DOPA)
4. X = ^{18}F, 6-Fluoro-3,4 dihydroxypheylalanine (FDOPA)

Figure 2. Structures of glucose, 3,4-dihydroxyphenylalanine, and their respective fluoro analogues.

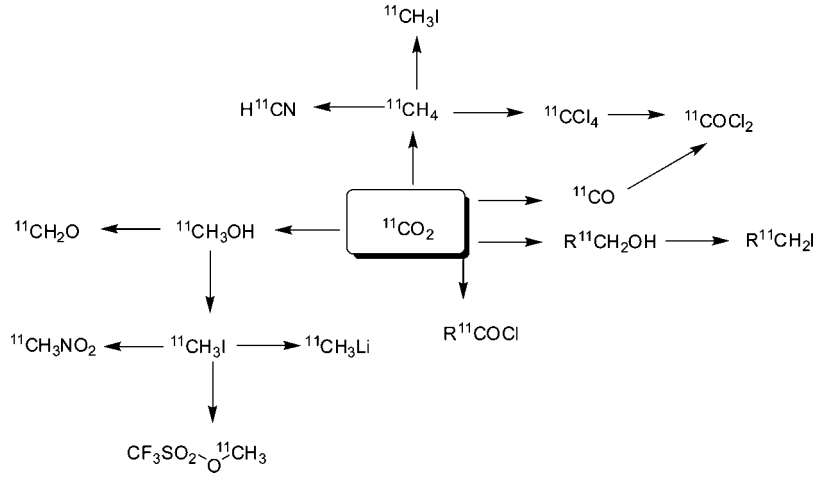

Figure 3. Pathways to carbon-11 reagents.

2. Radiolabeling Strategies

The relatively short physical half-lives of the positron-emitting nuclides require that the synthesis time for a PET imaging probe is kept as short as possible. Ideally, the synthesis and purification period should not exceed 2 to 3 times the physical half-life of the radionuclide in use, and strategies for the radiolabeling should aim to introduce the label in the synthetic sequence as late as possible. Multistep syntheses may be employed for complex molecules that require labeling via prothestic groups or have sensitive functional groups that need to be protected and deprotected after the radiolabeling. Usually a large excess of unlabeled precursor typically about 10^3- to 10^4-fold of the radioactive reagent is employed during the radiosynthesis to help drive the radiolabeling reaction to completion. This unusually high stoichiometric ratio results in pseudo-first-order reaction kinetics, which leads to an increased reaction rate and a rapid turnover of the radiolabeling entity. Practical reaction times vary and range from 1 to 30 min depending on the physical half-life of the radioisotope in use. Reaction volumes are typically 0.2–1 mL, and reaction temperatures also vary from ambient room temperature to 190 °C. Besides conventional heating, other techniques of reaction activation, for example, microwave heating, are also employed for radiochemical reactions. In fact, microwave heating has been shown to be effective in that faster, cleaner, and more selective reactions were obtained compared to conventional heating.[15]

Microfluidic devices have also recently been reported to show great potential for the radiolabeling of [^{18}F]FDG[16] and a range of other PET radiopharmaceuticals.[17] Distinct advantages of the microreactor technology include enhanced reaction kinetics and the possibility to work with smaller quantities of reagents and solvents on a nanoliter scale. It is remarkable that 2–3-fold higher radiochemical yields are obtained with shorter synthesis time relative to conventional radiosynthesis. It is expected that microfluid-based radiosyntheses will gain wide acceptance soon in the PET chemistry community.

All PET radiopharmaceuticals whether for human or animal use should show a high level of radiochemical purity (typically >95%), which is most frequently achieved by high-pressure liquid chromatography (HPLC) purification. In some cases, the use of disposable cartridges is sufficient enough to achieve highly purified radiolabeled compounds. Since PET radiopharmaceuticals are administered mainly by the intravenous route, it is important to check for sterility and apyrogenicity and all other quality control parameters that may have an adverse effect on an animal or a human subject under study.

2.1. Strategies for Carbon-11 Radiolabeling

A wide range of nuclear reactions exist for the production of ^{11}C, but the most commonly used method is the bombardment of a nitrogen gas target with protons according to the ^{14}N(p,α)^{11}C reaction.[18,19] A large number of ^{11}C radiolabeling precursors exist, but not all have found large-scale application in the routine labeling of biomolecules. Most can be produced directly in the target or obtained via chemical reactions from either $^{11}CO_2$ or $^{11}CH_4$. For example, the addition of oxygen (20 to 20 000 ppm) or hydrogen (5–10%) to the nitrogen target gas gives $^{11}CO_2$ or $^{11}CH_4$, respectively. With current available ^{11}C-radiolabeling techniques, $^{11}CO_2$ is the most versatile primary labeling precursor. In Figure 3 is shown a selection of ^{11}C-labeled precursor reagents that are derived from $^{11}CO_2$.

The most widely used ^{11}C-labeled precursor reagent, ^{11}C-methyl iodide, was developed some 30 years ago using the so-called "wet" method (Figure 4).[20]

More recently, an alternative approach known as the "gas phase" or "dry" method has been reported.[21,22] The synthetic approach depicted in Figure 5 has the advantage that it delivers ^{11}C-labeled PET imaging probes with higher specific

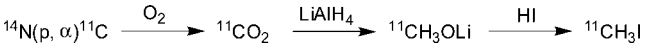

Figure 4. "Wet" method for the preparation of carbon-11 labeled methyl iodide.

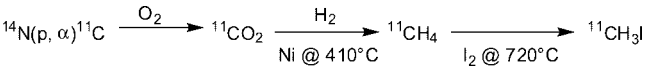

Figure 5. "Gas phase" method for the preparation of carbon-11 labeled methyl iodide.

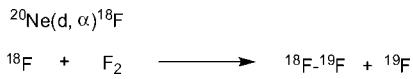

Figure 6. Method for the preparation of electrophilic $^{18}F_2$.

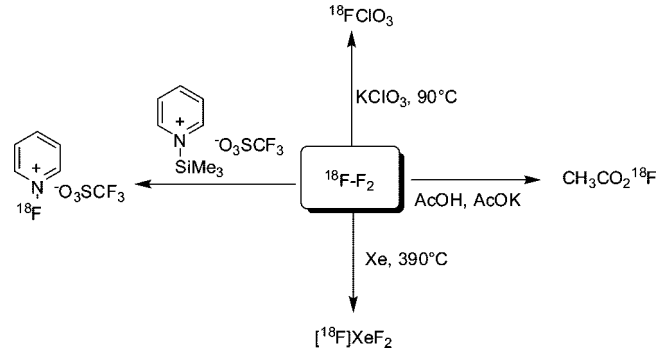

Figure 7. Pathways to some electrophilic ^{18}F-labeled reagents.

radioactivity relative to the "wet" method and is gradually becoming the method of choice in most PET chemistry laboratories. Besides ^{11}C-methyl iodide, ^{11}C-methyl triflate[23] has been utilized to improve the radiochemical yields in ^{11}C-methylations.

In general, most methylation methods applied in basic organic chemistry can be utilized in PET radiochemistry. A vast majority of ^{11}C-labeled imaging probes have been prepared either by N-, O-, or S-methylations, but in recent times $^{11}C-C$ coupling reactions using Stille, Suzuki, or Sonogashira cross-coupling reactions have also emerged.[24–27]

The theoretical maximum achievable specific radioactivity for ^{11}C-radiolabeled imaging probes is 3.4×10^5 GBq/μmol (Table 1). In practice, however, this value is never reached due to isotopic dilution from impurities such as nonradioactive CO, CO_2, CH_4, and other sources of carbon. For human studies, a specific radioactivity greater than 74 GBq/μmol is sufficient for most molecular probes used for the PET investigation of receptors, enzymes, and transporters in the CNS. Molecular imaging studies in small laboratory animals require higher specific radioactivities. Additional discussion on specific radioactivity is provided in section 3.2.

2.2. Strategies for Fluorine-18 Radiolabeling

As mentioned earlier, fluorine-18 is the most important positron-emitting isotope for PET imaging. Its optimal physical half-life of 110 min allows for multistep radiosynthesis, longer *in vivo* investigation, and above all commercial distribution to other clinical PET centers that lack a radiochemistry laboratory. Several nuclear reactions are known for the production of fluorine-18, and different target materials are used depending on the chemical form of the ^{18}F required.[28] Both the electrophilic and nucleophilic forms of ^{18}F are needed to satisfy the current need for ^{18}F-labeled pharmaceuticals.

2.2.1. Electrophilic Radiofluorinations

For electrophilic reactions, elemental ^{18}F-labeled fluorine ($^{18}F_2$) and its secondary derived precursors are used. The original method for the production of $^{18}F_2$ proceeds via the bombardment of a target gas consisting of neon and typically 0.1% unlabeled $^{19}F_2$ gas with deuterons according to the reaction depicted in Figure 6.

A more recent approach utilizes the $^{18}O(p,n)^{18}F$ reaction employing enriched $^{18}O_2$ as the target material.[29] Due to its high reactivity, $^{18}F_2$ is generally converted into less reactive and more selective ^{18}F-labeled fluorination agents such as acetyl hypofluorite,[30] xenon difluoride,[31] and fluorosulfonamides.[32] In Figure 7 are shown some of the ^{18}F-labeled fluorination agents derived from $^{18}F_2$. Besides ^{18}F-labeled acetyl hypofluorite, $^{18}F_2$ has found a wide application in the radiosynthesis of a number of ^{18}F-labeled PET imaging probes including [^{18}F]FDOPA (Figure 8), which ranks after [^{18}F]FDG in frequency of clinical use thanks to a regioselective demetalation reaction involving an aryltrimethyltin precursor and $^{18}F_2$.[33] For the radiolabeling reactions involving $^{18}F_2$, the maximum achievable radiochemical yield can only be 50%.

This is due to the fact that only one of the fluorine atoms in $^{18}F_2$ carries the ^{18}F label (Figure 6). Another shortcoming of the electrophilic labeling method is the low specific radioactivities of the final ^{18}F-labeled products. The low specific radioactivity values stem from carrier (i.e., unlabeled $^{19}F_2$ gas) addition, which is required for the recovery of $^{18}F_2$ from the surface of the target wall. Values for the specific activities obtained by this method are generally less than 0.40 GBq/μmol, and compounds prepared by the electrophilic method are thus not suitable for PET investigations involving saturable brain receptors due to their low concentrations. A recent attempt to improve the specific radioactivity via electric gaseous discharge of ^{18}F-labeled methylfluoride prepared from the no carrier added (nca) (i.e., no intentional addition of unlabeled fluoride) nucleophilic substitution method (Figure 9) gave final products with specific radioactivities in the range 10–20 GBq/μmol but still not high enough for brain receptor studies.[34] For PET studies requiring high specific radioactivities, the nca nucleophilic substitution reaction based on nca ^{18}F-fluoride is the method of choice.

2.2.2. Nucleophilic Radiofluorinations

The primary nca ^{18}F-fluoride ion obtained in an aqueous solution is produced by irradiation of oxygen-18 enriched water according to the $^{18}O(p,n)^{18}F$ reaction. Depending on the cyclotron and type of target body used, quantities of ^{18}F-fluoride radioactivity greater than 100 GBq can be achieved after 1 h of bombardment. Fluoride ion in aqueous medium is a poor nucleophile and inactivated for nucleophilic substitution reactions; therefore reactions involving nca ^{18}F-fluoride ion require strict exclusion of water. Activation of the ^{18}F-fluoride ion is achieved by applying cryptands in combination with alkali salts or tetra-*n*-butylammonium cation. The alkali (K, Cs, Rb) or quaternary ammonium salts are readily obtained from their respective carbonates, bicarbonates, or hydroxides, respectively. The most commonly used cryptand in combination with potassium carbonate is the aminopolyether Kryptofix 2.2.2. complex.[35,36]

Nucleophilic substitution reactions are performed mainly in dipolar aprotic solvents. For aliphatic systems the reaction mechanism proceeds via an S_N2 mechanism, and most often

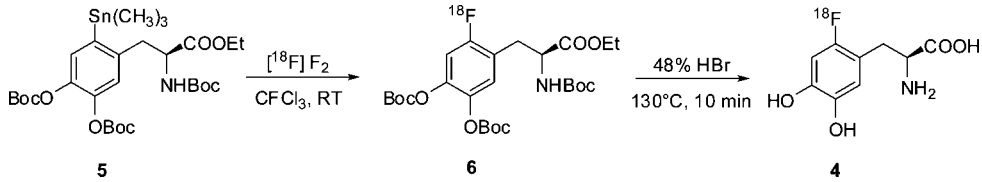

Figure 8. Electrophilic radiosynthesis of [^{18}F]FDOPA.

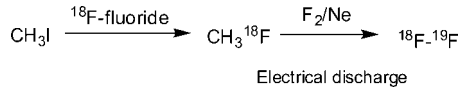

Figure 9. Preparation of $^{18}F_2$ using gaseous electrical discharge.

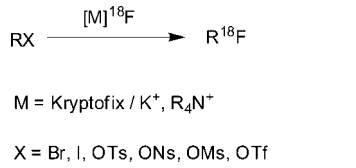

Figure 10. Nucleophilic aliphatic substitutions.

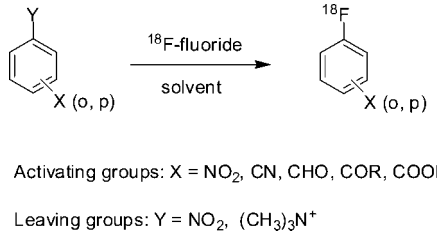

Figure 11. Nuclephilic aromatic substitutions.

precursors bearing bromo, iodo, tosylate, nosylate, and sulfonate as leaving groups are employed (Figure 10). Acetonitrile is the preferred solvent for nucleophilic substitutions on aliphatic systems, although sometimes dimethyl sulfoxide or dimethylformamide may be considered. Competing reactions, e.g., eliminations or degradations, due to the basicity of the reaction media may influence the radiochemical yields. Recent results showed that the addition of *tert*-butanol to acetonitrile could dramatically improve the radiochemical yields for certain aliphatic systems, and radiochemical yields as high as 80% were obtained.[37] Ionic liquids that have good thermal stability are alternatives to the above-mentioned solvents. A further advantage of using ionic liquids as solvents is the fact that nca ^{18}F-radiolabeling reactions can be carried out in the presence of water.[38]

Aromatic nca ^{18}F nucleophilic substitutions are feasible only if activated aromatic systems are employed. Strong electron-withdrawing substituents such as CN, CHO, NO_2, COOR, and RCO in *ortho* or *para* position are suitable for activation (Figure 11), and leaving groups are typically nitro and trimethylammonium salts.[39,40] Nca nucleophilic substitution reactions involving heterocyclic aromatic systems such as the electron-poor pyridine series, however, do not necessarily require activating groups, as shown in several publications[41–43] and a recent review by Dollé.[44] Dimethyl sulfoxide is the preferred solvent for aromatic nucleophilic substitutions, although sometimes dimethylformamide is useful.

In recent years, efforts have been directed toward finding new synthetic approaches to radiolabel biomolecules that do not bear activated aromatic moieties. Encouraging results have been achieved using diaryliodonium salts as precursors for simple molecules,[45,46] but the aromatic nca nucleophilic substitution of more complex molecules using diaryliodonium salts remains a challenge.[47] Decarbonylation of 2-[^{18}F]fluorobenzaldehydes has also been employed to prepare nonactivated ^{18}F-labeled aromatic systems.[48]

In general, complex molecules such as oligonucleotides, peptides, and antibodies are not amenable to direct fluorination with nca ^{18}F-fluoride ion due to denaturing of sensitive organic substrates and the presence of reactive functional groups such as free amino, carboxylic acid, or other CH-acidic functionalities.[49] Methods have been developed that employ nca ^{18}F-labeled small organic molecules called prosthetic groups, which are then chemoselectively coupled to the oligonucleotide, peptide, or antibody.[50–59] Typically, the ^{18}F-labeled prosthetic groups are incorporated into biomolecules via alkylation, acylation, amidation, or photochemical reactions.[60,61] In Figure 12 are shown some selected labeled prosthetic groups commonly used for labeling peptides and antibodies. A shortcoming of the use of prosthetic groups is the fact that the synthetic methods are comprised of multistep radiosyntheses and the radiolabel is incorporated very early in the synthesis sequence. To circumvent this shortcoming, new synthetic strategies for the direct labeling of peptides and other large molecules are currently being pursued. In a recent communication from our group,[62,63] peptides were radiofluorinated in a one-step nucleophilic substitution reaction. A general approach for the one-step nca fluorine-18 labeling of the peptides is shown in Figures 13 and 14. A recent study also demonstrated the feasibility of labeling organoboron and organosilicon bioconjugates with ^{18}F in a single step.[64] Expectations are that these newly developed methods would make the use of ^{18}F-labeled prosthetic groups in some cases redundant. An interesting approach that uses enzyme systems to label large biomolecules under mild conditions has also been described and shows prospect for the future.[65] For a collection of review articles on labeling strategies with positron-emitting nuclides see Schubiger et al.[66]

The nucleophilic method is the method of choice for the syntheses of ^{18}F-labeled radiopharmaceuticals with high specific radioactivity. Practical values for ^{18}F-labeled PET imaging probes using nca ^{18}F-fluoride are generally in the range 50–500 GBq/μmol, but the maximum theoretical achievable specific radioactivity of 6.3×10^4 GBq/μmol (Table 1) is never achieved due to isotopic dilution from water, solvents, reagents, and transport lines as previously discussed for carbon-11. Generally, although the theoretical specific radioactivity for carbon-11 is higher than that of fluorine-18 (Table 1), in practice specific radioactivities obtained for nca ^{18}F-labeled compounds are much higher. This results from the fact that fluorine is less ubiquitous in nature than carbon.

Recently, "click chemistry" has been applied in PET chemistry to prepare ^{18}F-labeled compounds. The application of the method is in its infancy, but it also shows great promise for preparing ^{18}F-labeled compounds with diversified substitutions.[67]

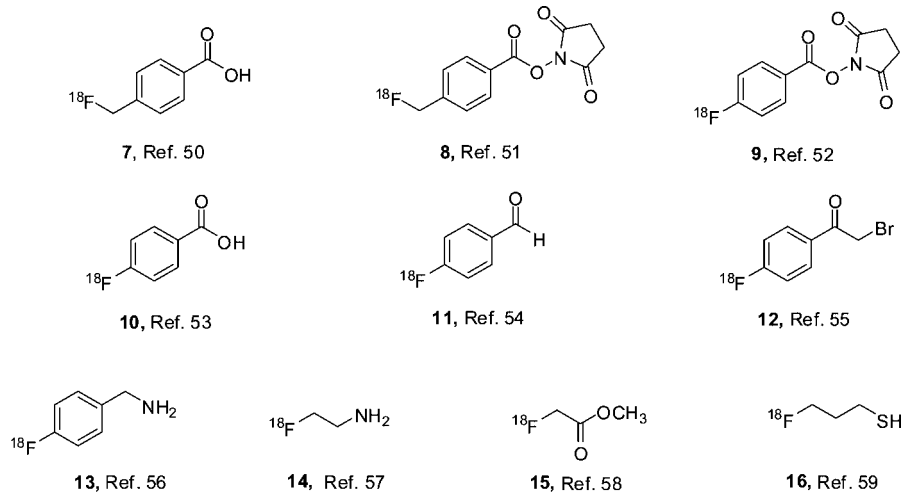

Figure 12. Examples of some prosthetic groups.

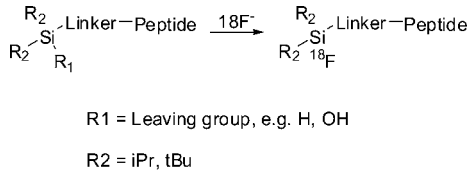

Figure 13. Direct nca nucleophilic fluorine-18 labeling of peptides.

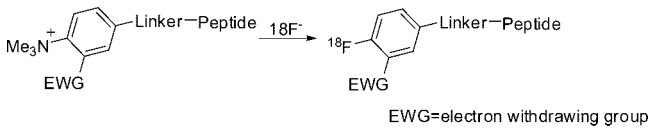

Figure 14. Direct one-step nca aromatic nucleophilic F-18 labeling of peptides.

3. Prerequisites for CNS PET Imaging Probes

Establishing the usefulness of a PET imaging probe for human applications requires the expertise of several scientists including radiochemists, pharmacologists, and clinicians who work in close collaboration in an interdisciplinary environment. For PET imaging probes to be useful as *in vivo* imaging agents, a number of prerequisites have to be fulfilled. Some of these prerequisites derived from several years of empirical research are briefly discussed below. Although these prerequisites represent a simplification of complex biochemical processes, they provide useful guidelines for designing molecular probes with improved probability of success.

3.1. Selectivity/Affinity for the Receptor

The equilibrium dissociation constant (K_d) of a drug receptor complex is the concentration of drug that occupies or binds to 50% of available receptor population. By definition, affinity is the reciprocal of equilibrium dissociation constant and is ideally highest for the target site to be imaged. Considering that the B_{max} (maximum concentration of binding sites) for most brain receptors is rather low (nano- to femtomoles per milligram tissue), PET imaging probes should have binding affinities in the subnanomolar range. But too high an affinity can render a PET radiopharmaceutical unsuitable because its uptake may become blood flow dependent instead of being dependent on the rate of binding. The uptake may essentially be irreversible, and equilibrium studies may not be possible. The K_d and B_{max} values are measured by *in vitro* equilibrium binding assays and are related to the labeled probe and the target protein, respectively. The receptor densities, for example for the dopamine D_2 receptor subtype, are on the order of 10 to 30 pM, and typical affinities of PET radioligands used for this target are in the range 1 to 10 nM. The *in vitro* B_{max}/K_d ratio, called the "binding potential", is often used to predict *in vivo* target to nontarget ratio, but the values for this ratio are only estimates for the *in vivo* situation. Typically, the *in vivo* binding potential is several-fold lower than the *in vitro* measured binding potential. This point has been highlighted in a recent editorial by Eckelman et al.[68]

3.2. Specific Radioactivity

Specific radioactivity (SA) refers to the amount of radioactivity per unit mass of a radiolabeled compound. The theoretical maximum SA of a radionuclide is a function of the physical half-life of the radionuclide and is calculated using the following equation:

$$SA = (\ln 2/t_{1/2})N \quad (1)$$

where N is the number of atoms of the radioactive element and $t_{1/2}$ is the physical half-life of the radionuclide. N can be converted to the equivalent number of moles by dividing by Avogadro's number (6.023×10^{23} atoms/mol). The theoretical maximum SA is simply then calculated from

$$SA(Bq/mol) = 1.16 \times 10^{20}/t_{1/2} \quad (2)$$

($t_{1/2}$ = half-life in units of hours).[69] It is obvious from this equation that the radionuclide with the shortest half-life would have the highest SA value. Thus in Table 1, oxygen-15, with the shortest half-life of 2 min, has the highest theoretical specific radioactivity. The relatively short half-lives of the PET isotopes result in low masses. For example, typical clinical doses of 370 MBq of ^{11}C and ^{18}F are equivalent to 1.186×10^{-11} and 1.0529×10^{-9}g, respectively. Therefore, the contribution in terms of mass of the radionuclides is negligible. The higher masses obtained after the radiosyntheses for the ^{11}C- and ^{18}F-labeled imaging probes, typically in the range 5–10 μg, result from contamination with stable isotopes ^{12}C and ^{19}F. For *in vivo* brain receptor imaging, PET radiopharmaceuticals must be prepared in high specific radioactivities so that only a small percentage of the total number of available binding sites is

occupied by the radioligand. Low specific radioactivity may lead to a significant saturation of the binding sites, which is associated with deterioration of signal-to-noise ratios, and depending on the target and its effector system, it may result in pharmacological or toxic effects. It should, however, be noted that during radioligand development an escalating dose of the unlabeled compound or other competing agents are used to saturate the binding sites in order to determine the specificity of the radiopharmaceutical in question.

3.3. Metabolism and Position of Label

Since PET cannot discriminate between signals from parent radioligand and radiolabeled metabolites, it is essential that PET ligands do not undergo rapid metabolism over the period of PET measurements. It has therefore to be verified that metabolites that are formed in the course of data acquisition do not contaminate the PET signals of the intact parent compound. This is usually determined in metabolite analysis using brain extracts from mice or rats. HPLC analysis of blood samples provides useful information on the clearance of the radiopharmaceutical, and useful PET ligands have less than 80% metabolism at the end of the PET imaging studies.

The position of the radiolabel in a molecule is a crucial factor and has to be considered very carefully during the planning of the synthetic approach since the loss of the radiolabel in a molecule by metabolic degradation will limit its usefulness as a PET ligand.

3.4. Blood−Brain Barrier Permeability

A source of failure for CNS PET imaging probes is often, besides the high nonspecific binding *in vivo*, the inability of the compounds to cross the blood−brain barrier (BBB). In assessing whether a radiopharmaceutical may undergo a lipid-mediated transport across the BBB, two important factors need to be taken into consideration: (a) the extent of hydrogen bond formation of the drug with water and (b) the molecular weight of the drug or radiopharmaceutical. As a general rule, hydrogen bond formation should be minimal and the total number of hydrogen bonds a drug forms with water should be less than eight to ten.[70] This explains also why peptide-based radiopharmaceuticals that have high levels of hydrogen bonding do not penetrate the BBB to any considerable extent. The molecular weight, which is a measure for molecule volume, should be below the 400–600 Da threshold. Excellent reviews are available that describe *in silico*,[71] *in vitro*,[72] and *in vivo*[73] methods for predicting BBB penetration. For PET radiopharmaceuticals, besides computational methods, the octanol/water partition coefficient, P, is quite often used as a predictor for BBB penetration, and log P values between 2 and 3.5 are generally considered optimal. Within a class of structurally related compounds, higher log P values generally translate into higher nonspecific binding. The discussion here holds for diffusion-mediated transport systems but not for specialized active transport systems such as amino acids or sugars. Furthermore, it has to be verified that the CNS imaging agent is not a substrate for P-glycoprotein (Pgp), which operates at the BBB. The development of mdr-1 knockout mice has made possible the assessment of the influence of Pgp on CNS molecular probes.

3.5. Clearance Rate, Protein Binding, and Nonspecific Binding

Also of importance are rapid clearance rates from blood and nonspecific binding sites (i.e., binding to nontarget sites). A low binding of radioligand to plasma proteins is essential since only the free fraction of radioligand in plasma is available for diffusion out of the vascular space. The nonspecific binding of the radiopharmaceutical under investigation must be low in order that a high target to background ratio can be achieved.

As mentioned earlier, these prerequisites do not provide a guarantee for a successful CNS PET radiopharmaceutical, these are only useful guidelines. It should be stressed at this point that an excellent drug performing well on the market is not necessarily a good molecular imaging agent. For example, the antidepressant fluoxetine (Prozac), one of the "blockbusters" on the pharmaceutical market, is as a PET radioligand not suitable for the imaging of the serotonin transporter due to high nonspecific binding *in vivo*.[74]

4. Molecular Imaging Probes for the CNS

4.1. Imaging Probes for the Dopaminergic Neurotransmission

The involvement of the dopaminergic system in numerous brain disorders such as schizophrenia, Parkinson's disease, and other movement disorders has prompted an intense research in this field. Five dopamine receptor subtypes (D_1-D_5) are known from cloning studies[75,76] and classified in two different families. The D_1 family includes the D_1 and D_5 subtypes, while the D_2 family consists of D_2, D_3, and D_4 subtypes. Substantial efforts have been directed toward the development of molecular imaging probes for the D_1 and D_2 subtypes in part due to their relative abundance in the striatum. The B_{max} values for the D_1 and D_2 receptors in the striatum are 50 pmol/g tissue and 20 pmol/g tissue, respectively.[77] Initial radioligand development work concentrated on the D_2 receptor subtype, and the types of compounds evaluated were structurally derived from butyrophenone and substituted benzamides. It is therefore no surprise that the first receptor to be visualized in the human brain was the D_2 receptor subtype using the butryophenone derivative [^{11}C]3-N-methylspiperone as the PET imaging agent.[78] Butyrophenones, however, have a disadvantage in that they lack selectivity. Besides the D_2 receptor subtype, they bind also with high affinity to 5-HT_2 (5-hydroxytryptamine subtype 2) receptors. The binding is essentially irreversible and does not allow equilibrium studies. Fortunately, the benzamide derivatives are more selective and show reversible binding. Of all the benzamide derivatives reported to date, [^{11}C]raclopride (Figure 15) is the most widely used routine PET ligand for the investigation of striatal D_2/D_3 receptors in humans.[79] [^{11}C]Raclopride has been used to image D_2/D_3 receptors in patients with Parkinson's disease, Huntington's disease, and schizophrenia, for determining receptor occupancy of antipsychotic drugs as well as for the indirect measurement of dopamine concentrations in the synaptic cleft.[80–83] [^{18}F]Fallypride[84] and [^{11}C]FLB 457,[85] also structural analogues of raclopride, have been used for the *in vivo* visualization of striatal and extrastriatal D_2 receptors, respectively.

For the D_1 receptor system, [^{11}C]SCH23990[86] and [^{11}C]NNC112[87] are in use for assessing the D_1 receptor

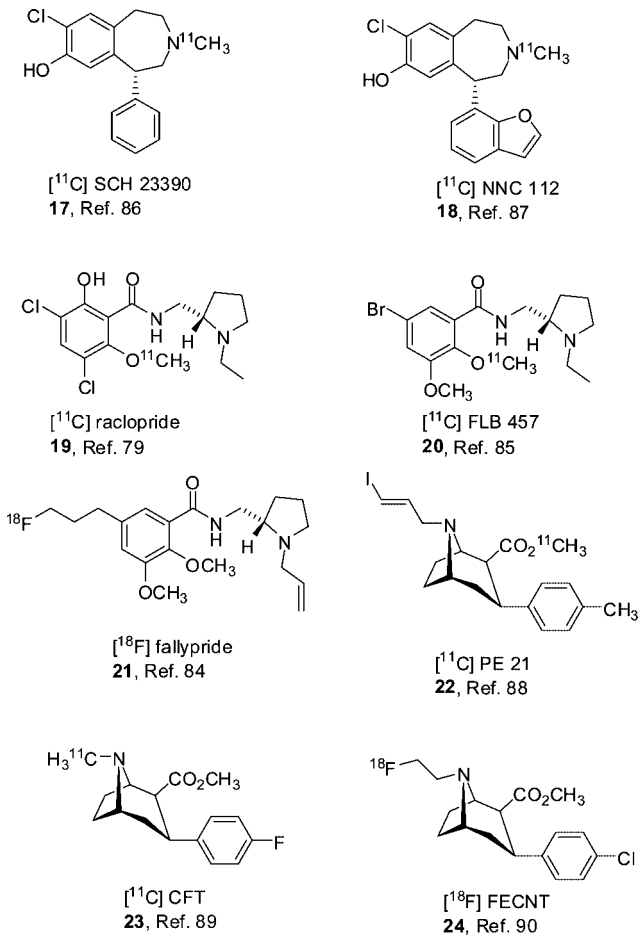

Figure 15. Structures of some established dopaminergic imaging probes.

density in Parkinson's patients, bipolar effective disorders, and schizophrenia as well as investigating the binding of neuroleptic drugs to the D_1 receptor. There are currently no selective PET radioligands for the dopamine D_3 and D_4 receptor subtypes.

For the presynaptic dopamine transporters (DATs), a series of cocaine congeners labeled with either ^{11}C or ^{18}F have been developed. Some of these compounds including [^{11}C]PE21,[88] [^{18}F]β-CFT,[89] and [^{18}F]FECNT[90] have found routine application in the clinics for assessing DAT density, which is altered in parkinsonian patients. In addition to being useful as diagnostic agents, these DAT PET ligands have also been employed as surrogate markers in the development of novel drugs for use in the therapy of brain disorders in which the dopaminergic system is implicated.

[^{18}F]6-Fluoro-L-DOPA has been used extensively to investigate presynaptic neuronal degeneration of the dopaminergic system, specifically the capacity of the neurons to synthesize dopamine. It passes the BBB through an active transport mechanism and is transformed to [^{18}F]6-fluorodopamine by neuronal aromatic amino acid decarboxylase (AADC).[91] A significant decrease in the uptake of [^{18}F]6-fluoro-L-DOPA, indicating a decrease in the density of the presynaptic dopaminergic nerve terminals, has been demonstrated in several PET studies (for a review see Piccini).[92] The metabolically more stable [^{18}F]6-fluoro-L-*m*-tyrosine, which is not a substrate for catechol-*O*-methyltransferase (COMT), has also been applied to study AADC activity.[93]

PET radioligands such as [^{11}C]clorgyline and [^{11}C]deprenyl are available for the investigation of monoamino oxidase

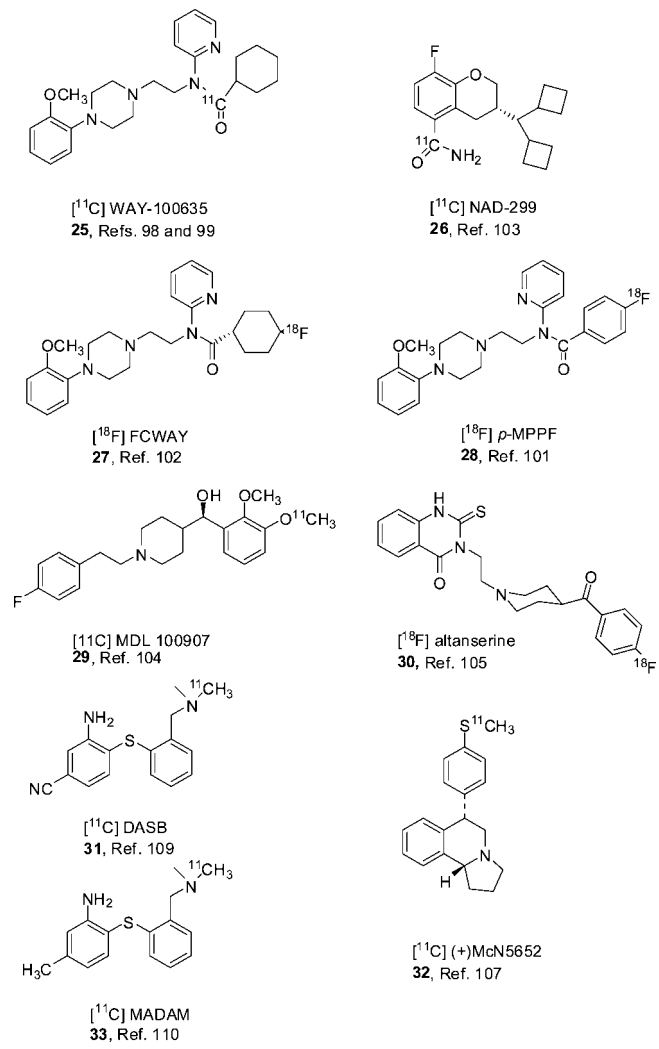

Figure 16. Some examples of serotonergic imaging probes.

A (MAO-A) and B (MAO-B), respectively.[94] PET studies with [^{11}C]clorgyline and [^{11}C]deprenyl have shown that smokers have approximately 25% and 40% reduction in MAO-A[95] and MAO-B,[96] respectively, and it is speculated that this reduction may account for the reduced rate of Parkinson's disease in smokers.[97]

4.2. Imaging Probes for the Serotonergic Neurotransmission

The serotonergic system has also been implicated in a number of neurological and psychiatric disorders such as depression, anxiety, schizophrenia, and Alzheimer's disease. Although more than 16 receptor subtypes for this system are known, PET imaging probes exist only for the 5-HT_{1A} and 5-HT_{2A} receptor subtypes, which are found in high densities in the hippocampus and neocortical regions of the brain. Examples of some established imaging agents for the serotonergic neurotransmission are shown in Figure 16. [^{11}C]WAY100635 labeled in the carbonyl position was shown to have high selectivity for the 5-HT_{1A} receptor subtype in humans, and its use in PET studies to assess receptor occupancy of a typical oral dose of pindolol, a 5-HT_{1A} receptor antagonist with beta-adrenoceptor antagonist properties, has also been demonstrated.[98,99] PET studies with [^{11}C]WAY100635 have also shown a reduced 5-HT_{1A} receptor density in patients with major depression.[100] Several

fluorinated analogues of WAY100635 including [^{18}F]p-MPPF[101] and [^{18}F]FCWAY[102] have also been prepared and evaluated as potential imaging probes for the 5-HT$_{1A}$ receptors. Robalzotan (NAD-299), a structurally different compound, has been labeled with carbon-11, and preliminary results show that [^{11}C]NAD-299 is a promising imaging probe for the 5-HT$_{1A}$ receptors.[103]

For the 5-HT$_{2A}$ receptor, PET imaging probes such as [^{11}C]MDL100907,[104] [^{18}F]Altanserin,[105] and [^{18}F]Setoperone[106] are in use.

The first promising tracer developed for the PET imaging of the serotonin transporter (SERT) was (+)[^{11}C]McN-5652.[107] Although (+)-[^{11}C]McN5652 labels the SERT in the human brain, it exhibits also high nonspecific binding and slow kinetics. Using (+)-[^{11}C]McN5652 as a SERT PET ligand a significant increase in the SERT density in the thalamus of patients with depression was observed.[108] More recently, a highly promising diarylsulfide class of compounds, namely, [^{11}C]DASB,[109] [^{11}C]MADAM,[110] and [^{11}C]HO-MADAM,[111] have been developed as putative PET ligands for the *in vivo* imaging of the SERT in humans.

4.3. Imaging Probes for the Cholinergic Transmission

The cholinergic system has also been implicated in a vast number of neurological and psychiatric disorders including depression and cognitive and memory disorders such as Alzheimer's and Parkinson's disease. Two main classes of acetylcholine receptors are known: nicotinic and muscarinic. Whereas the nicotinic acetylcholine receptors (nAChRs) are ligand-gated ion channels, the muscarinic acetylcholine receptors (mAChRs) are G-protein coupled receptors and operate via second messenger systems. PET ligands such as [^{11}C]4-NMPB,[112,113] [^{11}C]3-NMPB,[114,115] and [^{11}C]bezotropine[116] have been evaluated for the imaging of the muscarinic receptors, but all have a shortcoming in that they lack receptor subtype selectivity for the four receptor subtypes of mAChRs. PET studies with [^{11}C]4-NMPB demonstrated that normal aging was associated with a reduction in the density of muscarinic receptors in neocortical regions and thalamus.[113]

The nAChR exists as pentamers and comprises α, β, and other subunits. The most abundant nAChR in the mammalian brain is the $\alpha4\beta2$ subtype. [^{11}C]Nicotine was used in humans to image the nicotinic receptors, but the PET images were plagued with high nonspecific binding.[117,118] Recently, a number of PET imaging probes derived from epibatidine with high *in vivo* specific binding have been reported. Epibatidine itself and some of its analogues exhibited extremely high toxicity and were thus never used for human studies. Two nontoxic $\alpha4\beta2$ receptor subtype PET imaging probes, [^{18}F]-2-F-A-85380[119,120] and [^{18}F]6-A-85380,[121,122] are currently under investigation in human subjects. Recent data from these studies show that Alzheimer's[123] and Parkinson's disease[124] patients show a significantly reduced $\alpha4\beta2$ density and a good correlation with severity of disease.

[^{11}C]MP3A (*N*-methyl-3-piperidylacetate) and [^{11}C]MP4A (*N*-methylpiperidin-4-ylacetate) (Figure 17) have been investigated as potential PET imaging agents for visualizing central acetylcholinesterase activity in humans. PET studies in healthy controls and patients with Alzheimer's disease (AD) showed a widespread reduction of acetylcholinesterase activity in the cerebral cortex of AD patients.[125]

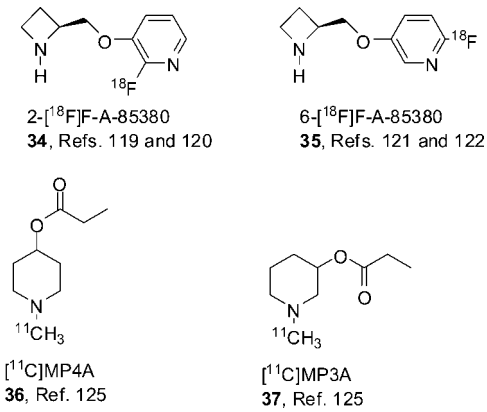

Figure 17. Some examples of cholinergic imaging probes.

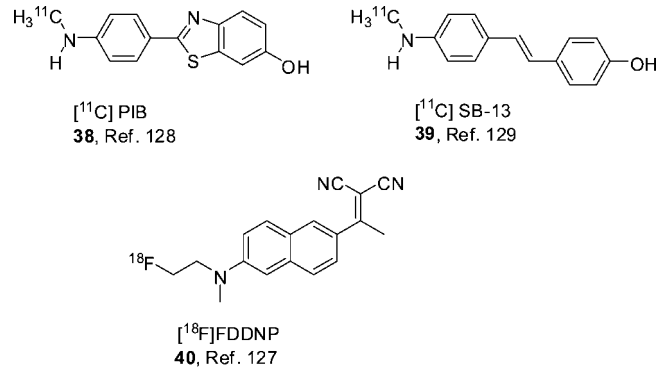

Figure 18. Structures of some beta-amyloid imaging probes.

4.4. Molecular Imaging Probes for the Imaging of β-Amyloid Load

The pathophysiology of Alzheimer's disease is an area of intense research. The β-amyloid peptides Aβ1-40 and Aβ1-42 are major metabolites of the amyloid precursor protein (APP) and are found in senile plaques and cerebrovascular amyloid deposits in AD.[126] Although the presence of extracellular amyloid-rich β-amyloid plaques and hyperphosphorylated tau filaments in intracellular neurofibrillary tangles (NFTs) is a common feature in the brain of patients with AD, the exact mechanisms leading to AD are not yet clear. The PET imaging of β-amyloid plaques will greatly improve the diagnosis of AD as well as accelerate the development of antiamyloid drugs currently under development provided appropriate imaging probes are available.

One of the first PET imaging probes (Figure 18) developed and investigated in humans was the lipophilic naphthalene derivative [^{18}F]FDDNP ((2-(1-{6-[(2-[^{18}F]fluoroethyl-(methyl)amino]-2-naphthyl}-2-ethylidene)malonitrile).[127] This compound was shown to bind to both β-amyloid plaques and NFTs and shows promise in differentiating mild cognitive impairment from healthy controls and patients with AD. A new compound, ^{11}C-labeled 6-OH-BTA ([*N*-methyl-[^{11}C]-2-[4′-(methylamino)phenyl]6-hydroxybenzothiazole), also known as Pittsburgh Compound B ([^{11}C]PIB), was reported recently, and its utility as a selective β-amyloid plaque imaging agent in patients with AD was also examined.[128] Highest binding for ^{11}C-labeled PIB was observed in the posterior cingulate, frontal cortex, and caudate nuclei, followed by lateral temporal and parietal cortex, and this uptake was higher in all the AD patients than in controls. The extent of [^{11}C]PIB uptake did not, however, correlate with dementia severity in Alzheimer's patients but matched

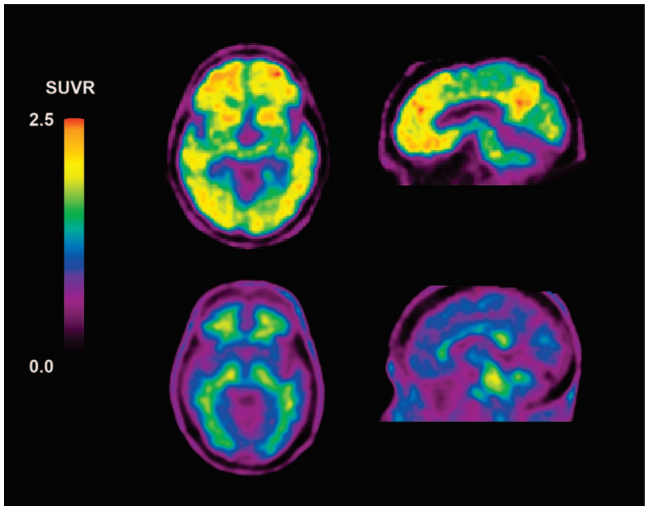

Figure 19. Transaxial and midsagittal PET images obtained 90–120 min postinjection of 300 MBq BAY 94-9172 in a 75-year-old subject with mild Alzheimer's disease (MMSE 26) and a 76-year-old healthy control. The color scale is set so that cerebellar white matter is green to yellow in both cases. The HC subject (bottom row) shows extensive white matter binding most apparent in the corpus callosum, peri-thalamic area, pons, and centrum semiovale. The AD subject shows cortical binding in frontal, posterior cingulate/precuneus, and lateral temporal areas with relative sparing of occipital and sensori-motor cortex. (Image provided by Chris Rowe, Austin Hospital, Nuclear Medicine & Centre for PET, Melbourne Australia).

histopathologic reports of β-amyloid plaque distribution in aging. A recent study using a ^{11}C-labeled compound, [^{11}C]SB-13, also demonstrated the feasibility of PET imaging of β-amyloid plaques in humans.[129] More recently, a new ^{18}F-labeled compound called [^{18}F]BAY 94-9172, which shows high affinity binding to β-amyloid plaques (Figure 19), has been shown to be useful for detecting β-amyloid load early in disease progression. The fact that significant β-amyloid was seen in a subgroup of clinically healthy elderly persons may be interpreted as recognition of presymptomatic AD, but this requires additional longitudinal studies.[130] In this study, FTLD (frontotemporal lobar degeneration) subjects show no gray matter retention of [^{18}F]BAY 94-9172. [^{18}F]BAY 94-9172 is thus so far the only fluorine-18 labeled β-amyloid imaging probe reported to date that discriminates well between AD and healthy controls and should facilitate integration of β-amyloid imaging into clinical practice. It is expected that the development of specific molecular imaging probes for β-amyloid imaging would give new insights into Alzheimer's disease progresssion.

4.5. PET Imaging Probes for the Glutamatergic Neurotransmission

Glutamate is considered the major excitatory neurotransmitter in the CNS. Its central effects are mediated through ionotropic and metabotropic glutamate receptors (mGluRs). The ionotropic glutamate receptors include NMDA (*N*-methyl-D-aspartate), AMPA (α-amino-3-hydroxy-5-methyl-isoxazole-4-propionate), and kainate receptors. The mGluRs are G-protein coupled receptors that activate intracellular secondary messenger systems when bound by the physiological ligand glutamate. Eight metabotropic glutamate receptor subtypes have been identified and classified into three groups. Group I mGluR (mGluRs 1 and 5) are coupled to phospholipase C and up/down-regulate neuronal excitability. Group II (mGluRs 2 and 3) and group III (mGluRs 4, 6, 7, and 8) inhibit adenylate cyclase and hence reduce synaptic transmission.[131]

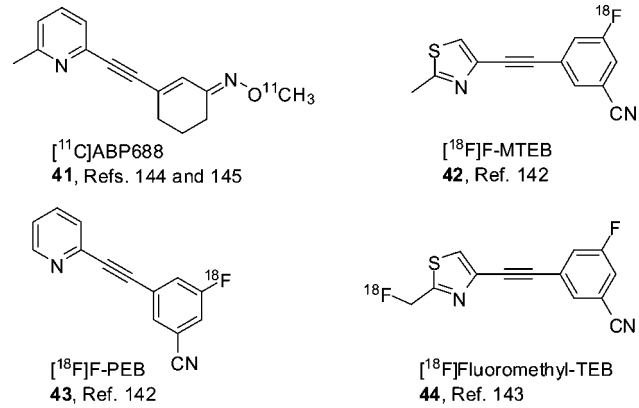

Figure 20. Structures of mGluR5 PET imaging probes currently under evaluation.

Over the course of the years, many attempts have been made by several research groups to develop PET molecular imaging probes for the ionotropic glutamate receptors due to their possible involvement in higher cognitive functions such as memory and learning, and a wide variety of brain diseases including anxiety,[132,133] depression,[132] schizophrenia,[134] Parkinson's disease,[135] drug addiction or withdrawal,[136] and various pain states.[137,138] But despite strenuous efforts, no suitable PET radioligand currently exists for the imaging of the ionotropic glutamate receptors.[139–141] Three new fluorinated compounds (Figure 20) for the PET imaging of the metabotropic glutamate receptor subtype 5 (mGluR5) have been described in two recent publications, but it is not clear yet whether these compounds can be used for the imaging of mGluR5 in humans.[142,143] Our group recently reported on a novel, selective, and high-affinity mGluR5 antagonist that shows promise as a PET radioligand for the imaging of the mGluR5 in humans.[144,145] This new compound, [^{11}C]ABP688 (Figure 20), displayed an *in vivo* distribution pattern in rodents and human subjects consistent with the known regional density of mGluR5. In Figure 21 is shown a PET image of [^{11}C]ABP688 uptake in a human brain showing the regional distribution of mGluR5. Ongoing clinical studies involving the use of [^{11}C]ABP688 would show the utility of this new molecular imaging agent in patients with psychiatric and neurological disorders.

5. Challenges in Small Animal PET Imaging

Although PET has been in use for more than 30 years now in neuroscience, most applications were in man and nonhuman primates. This was because the clinical PET imaging systems used for these studies were not capable of resolving small brain structures in rodents. The development of dedicated new small animal PET scanners with significantly improved spatial resolution has revolutionized molecular imaging in this field. But despite the fact that analogous PET studies can be carried out in small animals and in humans, small animal PET imaging poses a number of challenges.

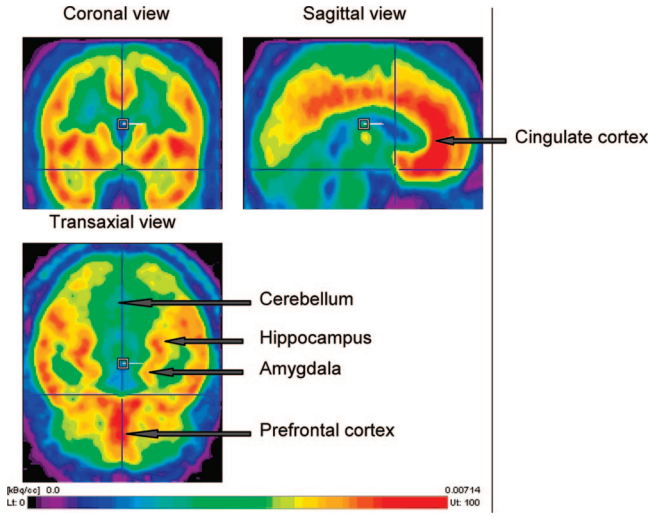

Figure 21. Uptake of [^{11}C]ABP688 in a healthy volunteer. High accumulation in mGluR5-rich brain regions such as cingulate cortex, amygdala, hippocampus, and prefrontal cortex is observed. The cerebellum, a brain area known to have negligible mGluR5 density, showed low radioactivity accumulation. Red color indicates highest activity concentrations and blue color lowest activity concentrations.

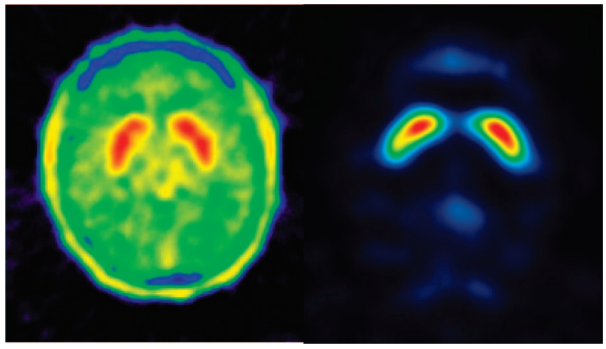

Figure 22. Horizontal sections through the brain of a human (left) and NMRI mouse (right) injected with [^{18}F]FDOPA and [^{18}F]fallypride, respectively. The human scan was undertaken using an Advance scanner (GE Medical Systems); the mouse scan was acquired on a dedicated small animal PET tomograph with ultrahigh resolution (quad-HIDAC; Oxford Positron Systems, UK). The color scale is arbitrary and not normalized. Red color indicates highest activity concentrations, blue and black color lowest activity concentrations.

5.1. Resolution versus Sensitivity of the PET System

Due to the different physical sizes of human and rodent brains, dedicated small animal PET cameras require a much higher resolution compared to clinical systems. Recent advances in detector technology have led to a substantial improvement in spatial resolution, permitting the resolution of tissue volumes smaller than 10 μL.[146] Such a volumetric resolution is sufficient to visualize and quantify a variety of molecular targets and biochemical processes in the major areas of the mouse and rat brain. Figure 22 exemplifies the comparable resolution and quality of a PET image visualizing dopaminergic neurotransmission in the striatum of a human and mouse brain. The striatum is a tiny structure in the mouse brain of less than 20 μL volume. Upon injection of the D_2 receptor ligand [^{18}F]fallypride, the resolution of the small animal PET camera permitted a clear-cut visualization of the mouse striatum.

A typical volumetric image resolution element (voxel) in small animal PET is below 1 μL. To preserve the number of registered counts per voxel and to obtain a comparable signal-to-noise ratio (S/N), preclinical systems should ideally have a much higher sensitivity compared to clinical systems. However, the sensitivity of small animal PET imaging systems is still limited. As a consequence, significantly higher doses of radioactivity have to be administered to a rodent to achieve a higher number of coincidence events detected from a rodent imaging voxel and to obtain similar count statistics to clinical PET studies. The requirement to inject higher doses of radioactivity into rodents, however, is correlated with the injection of a significant mass of cold compound per body weight. High occupancy or even saturation of the target protein by the radioligand may then lead to the deterioration of signal-to-noise ratios and—depending on the target and its effector system—to pharmacological or even toxic effects. Such a violation of the tracer principle impedes the use of kinetic modeling approaches and quantitative analysis of the PET data.[147]

5.2. Anesthesia

In contrast to human PET imaging, PET data collection in small animals must involve immobilization of the animal, which is usually attained by anesthesia of the animal during the PET scanning procedure. Several issues have to be considered to minimize the confounding influence of anesthesia on tracer kinetics and distribution. In general, anesthesia should be administered in a controllable manner and at a superficial level. The most established and consistent anesthetic regimen in small animal PET imaging involves isoflurane inhalation anesthesia of spontaneously breathing animals. Like isoflurane, most anesthetics have significant impact on the respiratory and cardiovascular systems, and consequently, tracer distribution and elimination will be influenced *in vivo* by the use of anesthesia. Cross-comparisons between anesthetized and nonanesthetized animals using alternative techniques (such as *post mortem* tissue sampling) must be performed to assess the effect of anesthesia on tracer accumulation. For example, the striatal concentrations of the radiotracer 6-[^{18}F]fluoro-L-*m*-tyrosine ([^{18}F]FMT) in the brain of anesthetized mice was 3-fold larger compared to nonanesthetized animals.[148] Such high discrepancies of tracer concentrations between anesthetized and nonanesthetized animals point to prominent *in vivo* metabolism of the radiotracer, thus complicating data interpretation and reducing the predictability of tracer characteristics in other species. Some anesthetics are also known to target neurotransmitter receptors or transporters in a direct or indirect manner. Isoflurane, for example, interacts directly with the $GABA_A$ receptor and was also shown to induce changes in the dopaminergic system in nonhuman primates, possibly by modulating presynaptic dopamine transporter availability.[149–151] Figure 23 demonstrates the influence of isoflurane anesthesia on striatal activity concentrations of [^{18}F]fallypride, a ligand binding to postsynaptic D_2 receptors. *Post mortem* activity concentrations in the striatum of anesthetized and nonanesthetized animals differed by only 20% at 63 min after injection excluding a substantial influence of isoflurane anesthesia on [^{18}F]-fallypride binding.[152]

Fluctuations in the anesthetic level among various scans is supposed to increase the interindividual variation in tracer

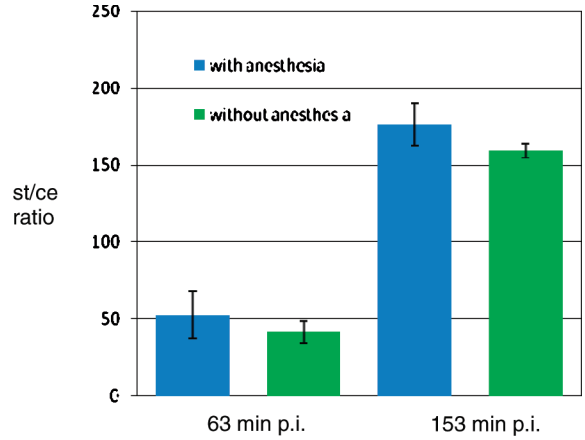

Figure 23. Striatal activity concentrations (normalized to the injected dose per body weight) of anesthetized and nonanesthetized mice injected with [^{18}F]fallypride and sacrificed at two different time points after injection.

uptake, kinetics, and metabolism and must be kept at a minimum by standardization of anesthetic regimens and precise monitoring of physiological and hemodynamic parameters. Homeostasis of fluid, electrolyte, and acid/base balance during anesthesia should be considered, especially for long-term scanning (>60 min). In addition, body temperature must be controlled and adjusted by a rectal probe and an appropriate heating device.

The compromising effects of anesthesia for PET imaging can be partly avoided for radiopharmaceuticals that are efficiently trapped in their target tissue and if no information about tracer kinetics is required. The animal is allowed to remain awake during the uptake and accumulation phase of the radiotracer and is only anesthetized when tracer uptake is complete and a steady state has been reached. [^{18}F]FDG is a good example of a tracer that may be used for such a static PET scanning protocol.[153] PET experiments with a complete omission of anesthesia will remain undoable for routine rodent scanning. Some PET experiments have been performed in conscious and trained cats or monkeys.[154–157] Recently, a nonanesthetized rat was trained to accept head fixation and scanned for 60 min.[158] With regard to animal welfare issues and scanning throughput, this approach will probably not achieve general acceptance. Furthermore, the effects of the physical and mental stress imposed on the animal by the active restraint are not well investigated. Alternatively, a PET system mounted to a rat's head permitted imaging of the conscious rodent brain,[159] but the practicability and utility of such an experimental approach has still to be proven.

5.3. Data Quantification

PET imaging using appropriate small animal models has emerged as a powerful technique to explore neurophysiology and neuropharmacology in a noninvasive and potentially highly quantitative manner. However, only limited information is currently available on the feasibility to achieve absolute quantification in small animal PET imaging. The new generation of dedicated small animal PET systems and the associated software packages have still not reached the standards and quantitative accuracy of state-of-the-art clinical PET systems. Corrections for attenuation in the animal's body as well as for scattered and random coincidences have to be included in the reconstruction software. Furthermore, calibration factors should be routinely determined and applied to allow conversion of scanner units (counts/voxel/s) to radioactivity concentrations (kBq/mL). Dynamically acquired and reconstructed PET data can be further processed and quantified by applying kinetic modeling approaches. To perform such fully quantitative dynamic PET experiments, the time course of tracer delivery to the tissue must be determined. This so-called arterial input function is a prerequisite for precise quantification of various biological parameters. Several techniques have been successfully applied in humans, but most of them have only limited applicability for routine work in rodents. Some of these techniques are invasive such as arterial microsampling of blood, arterial-venous shunts, and beta-probe measurements and are far from being routinely applied. Other techniques using image-based extraction of input functions (e.g., left-ventricle regions of interest) are characterized by a low degree of complexity and invasiveness and may be preferentially employed in future PET studies (for a review see LaForest et al.).[160]

Another prerequisite for reliable and precise quantitative PET imaging involves high intrastudy stability and interstudy reproducibility of the PET imaging experiment. Only a detailed standardized experimental protocol and standardized evaluation techniques avoid the introduction of bias to the analysis and permit drawing meaningful conclusions from a longitudinal study with repetitive PET scanning experiments. The maintenance of physiological and hemodynamic stability of anesthetized animals is one important criterion. The stability of the PET system represents another crucial point that must be controlled by regular performance tests and calibrations. The use of internal radioactive standards during each PET measurement might also help to monitor uniform system sensitivity during longitudinal studies. Standardization of acquisition and reconstruction protocols as well as calculation of standardized uptake values (SUV) may also allow a better comparison of PET data across studies or research institutions.

Small animal PET studies are typically analyzed by regions of interest (ROIs) drawn manually on the PET image. However, in the absence of any anatomical information ROIs are just based on the observed radioactivity distribution. Inconsistent drawing of ROIs within and across experimental series will thus introduce errors to a study. Contour-finding algorithms and coregistration of PET and CT images will probably facilitate ROI delineation and improve the accuracy of a ROI analysis. The use of stereotactic frames for brain studies guarantees a reproducible positioning of the animal's head and facilitates spatial alignment of PET images and their quantitative analysis by atlas-based approaches.[161]

The translatability of PET data obtained in mice and rats to the human setting is a great topic of discussion in the scientific community. There are considerable species differences in metabolism, protein binding characteristics, target site density, etc., and the prediction whether a successfully characterized PET tracer in rodents can be effectively used in humans is rather critical. Figure 24 exemplifies the highly variable uptake pattern of [^{18}F]FDOPA in a mouse and human brain. [^{18}F]FDOPA visualizes presynaptic integrity of dopaminergic synapses in the human striatum and has proven its utility in the clinical diagnosis of Parkinson's disease. When administered to mice, however, [^{18}F]FDOPA was found to distribute uniformly in the brain without specific accumulation in the striatum (Figure 24, right) despite the concomitant use of the inhibitors for the enzymes AADC

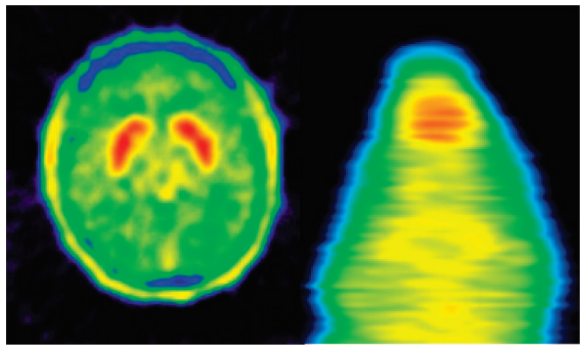

Figure 24. Comparison of representative horizontal PET images through the striatum of a healthy human (left) and a wild-type C57/BL6 mouse (right), both injected with the radiotracer [^{18}F]-FDOPA.

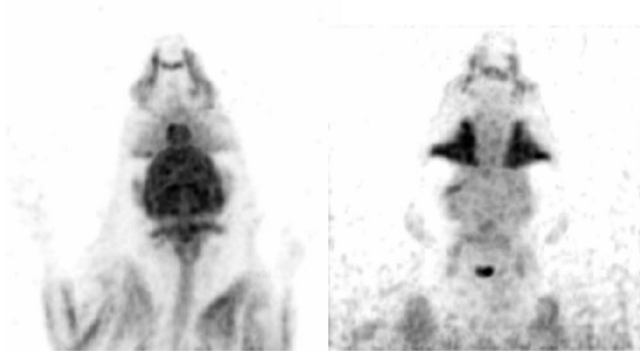

Figure 25. Comparison of maximum intensity projections (MIP) of the head of a Brown-Norway rat (left) and a Wistar rat (right), both injected with the radiotracer [^{18}F]FDG.

and COMT.[148] Hume and colleagues reported similar findings in the rat brain using [^{18}F]FDOPA, suggesting that rodent metabolism of [^{18}F]FDOPA might be too fast and efficient to allow for sufficient specific tracer accumulation in rodents.[162]

Considerable variations of PET tracer uptake and metabolismus may also occur among various strains of mice and rats. Strain differences in response to anesthetics or other pharmacologically active compounds are documented in rodents, but the impact of the genetic background of a specific rodent strain on radiotracer characteristics is less well described. Cerebral glucose metabolism assessed by intravenous administration of [^{18}F]FDG, for example, is strikingly variable in routinely used rat strains such as Brown-Norway and Wistar (Figure 25). As observed for many PET radiotracers, the nonspecific accumulation of [^{18}F]-FDG in intraorbital Harderian glands is also highly differing. In order to produce meaningful rodent data that can be reliably extrapolated to the human situation, these intraspecies variability in rodents must not be neglected.

6. Conclusion and Perspectives

Recent synthetic and technical developments have made possible the radiolabeling of imaging probes with carbon-11, fluorine-18, or other PET isotopes for preclinical research as well as for clinical applications. The increasing number of new targets and new molecular entities with complex structures will demand new radiolabeling strategies. The accomplishment of this goal is expected to eventually further harness the progress of PET as a powerful functional molecular imaging tool.

Numerous molecular imaging probes have been discussed here in this review, but for a vast majority of systems, such as the ionotropic glutamate receptors and norepinephrine transporters, no molecular imaging probes are available to aid in the diagnosis of diseases in which these proteins are up/down-regulated. Radiochemists and pharmacologists are therefore challenged to develop useful and selective PET imaging agents for neurotransmission systems lacking appropriate imaging probes. But one has to acknowledge that PET radiopharmaceutical development is not a straightforward process. It is an iterative process that requires a lot of effort and luck. One may follow all the guidelines and criteria needed for a CNS imaging probe, but there is no guarantee that a successful tracer for human application will be the end product, and obviously no successful radiopharmaceutical can fulfill all the requirements.

Small animal PET imaging is becoming an increasingly important methodology to analyze CNS functions in a noninvasive manner. Recent advances in PET imaging technologies allow addressing the same neurobiological questions in mice and humans. Obtaining consistent and quantitative PET images and data sets is one of the greatest strengths of rodent neuroimaging but also its greatest challenge. The next improvements with respect to scanner performance and data quantification are eagerly awaited. Integrating CT or MRI to PET has additional benefit of greater accuracy due to high-resolution anatomic imaging. Commercial small animal and clinical PET-CT systems are available, but the challenge now is to combine MRI and PET for routine CNS imaging in small animals because of the excellent soft tissue contrast of MRI. The future development, therefore, of *in vivo* PET in small animal brain imaging will equally be dependent not only on radiochemists and pharmacologists but also on the contributions made by physicists and engineers.

7. Acknowledgments

The authors would like to thank Dr. Linjing Mu for technical support.

8. References

(1) Haberkorn, U.; Eisenhut, M. *Eur. J. Nucl. Med. Mol. Imaging* **2005**, *32*, 1354.
(2) Weissleder, R.; Mahmood, U. *Radiology* **2001**, *219*, 316.
(3) Massoud, T. F.; Gambhir, S. S. *Genes Dev.* **2003**, *17*, 545.
(4) Doubrovin, M.; Serganova, I.; Mayer-Kuckuk, P.; Ponomarev, V.; Blasberg, R. G. *Bioconjugate Chem.* **2004**, *15*, 1376.
(5) Thakur, M.; Lentle, B. C. *Radiology* **2005**, *236*, 753.
(6) Mankoff, D. A. *J. Nucl. Med.* **2007**, *48*, 18N.
(7) Levin, C. S. *Eur. J. Nucl. Med. Mol. Imaging* **2005**, *32*, 325.
(8) Pauling, L. *Nature of the Chemical Bond*; Cornell University Press: New York, 1940; p 189
(9) Zhang, W.; Koehler, K. F.; Harris, B.; Skolnick, P.; Cook, J. M. *J. Med. Chem.* **1994**, *37*, 745.
(10) Leo, A.; Hansch, C.; Elkins, D. *Chem. Rev.* **1971**, *71*, 525.
(11) Garnett, E. S.; Firnau, G.; Nahmias, C. *Nature* **1983**, *305*, 137.
(12) Volkow, N. D.; Fowler, J. S.; Gatley, S. J.; Logan, J.; Wang, G. J.; Ding, Y. S.; Dewey, S. *J. Nucl. Med.* **1996**, *37*, 1242.
(13) Becherer, A.; Szabó, M.; Karanikas, G.; Wunderbaldinger, P.; Angelberger, P.; Raderer, M.; Kurtaran, A.; Dudczak, R.; Kletter, K. *J. Nucl. Med.* **2004**, *45*, 1161.
(14) Reivick, M.; Kuhl, D.; Wolf, A.; Greenberg, J.; Phelps, M.; Ido, T.; Casella, V.; Hoffmann, E.; Alavi, A.; Sokoloff, L. *Circ. Res.* **1979**, *44*, 127.
(15) Lasne, M. C.; Perrio, C.; Rouden, J.; Barré, L.; Roeda, D.; Dollé, F.; Crouzel, C. *Top. Curr. Chem.* **2002**, *222*, 203.
(16) Lee, C. C.; Sui, G.; Elizarov, A.; Shu, C. J.; Shin, Y. S.; Dooley, A. N.; Huang, J.; Daridon, A.; Wyatt, P.; Stout, D.; Kolb, H. C.;

Witte, O. N.; Satyamurthy, N.; Heath, J. R.; Phelps, M. E.; Quake, S. R.; Tseng, H. R. *Science* **2005**, *310*, 1793.
(17) Gillies, J. M.; Prenant, C.; Chimon, G. N.; Smethurst, G. J.; Perrie, W.; Hamblett, I.; Dekker, B.; Zweit, J. *Appl. Radiat. Isot.* **2006**, *64*, 325.
(18) Wolf, A. P.; Redvantly, C. S. *Appl. Radiat. Isot.* **1977**, *28*, 29.
(19) Ferrieri, R. A.; Wolf, A. P. *Radiochim. Acta* **1983**, *34*, 69.
(20) Comar, D.; Maziere, M.; Crouzel, M. *J. Labelled Compd. Radiopharm.* **1973**, *9*, 461.
(21) Larsen, P.; Ulin, J.; Dahlstrom, K.; Jensen, M. *Appl. Radiat. Isot.* **1997**, *48*, 153.
(22) Link, J. M.; Clark, J. C. *Nucl. Med. Biol.* **1997**, *24*, 93.
(23) Jewett, D. M. *Appl. Radiat. Isot.* **1992**, *43*, 1383.
(24) Anderson, Y.; Cheng, A. P.; Langström, B. *Acta Chem. Scand.* **1995**, *49*, 683.
(25) Samuelsson, L.; Langström, B. *J. Labelled Compd. Radiopharm.* **2003**, *46*, 263.
(26) Huang, Y. Y.; Narendan, R.; Bischoff, F.; Guo, N. N.; Zhu, Z. H.; Bae, S. A.; Lesage, A. S.; Laruelle, M. *J. Med. Chem.* **2005**, *48*, 5096.
(27) Wuest, F. R.; Berndt, M. J. *Labelled Compd. Radiopharm.* **2006**, *49*, 91.
(28) Qaim, S. M.; Clark, J. C.; Crouzel, C.; Guillaume, M.; Helmeke, H. J.; Nebeling, B.; Pike, V. W. ; Stöcklin, G. *Radiopharmaceutical for Positron Emission Tomography–Methological Aspects*; Kluwer: Dordrecht, 1993; p 1.
(29) Bishop, A.; Satyamurthy, N.; Bida, G.; Hendry, G.; Phelps, M.; Barrio, J. R. *Nucl. Med. Biol.* **1996**, *23*, 189.
(30) Fowler, J. S.; Shiue, C. Y.; Wolf, A. P.; Salvador, A. P.; MacGregor, R. R. *J. Labelled Compd. Radiopharm.* **1982**, *19*, 1634.
(31) Chirakal, R.; Firnau, G.; Schrobigen, G. J.; MacKay, J.; Garnett, E. S. *Appl. Radiat. Isot.* **1984**, *35*, 401.
(32) Satyamurthy, N.; Bida, G. T.; Phelps, M. E.; Barrio, J. R. *Appl. Radiat. Isot.* **1990**, *41*, 733.
(33) Namavari, M.; Bischop, A.; Satyamurthy, N.; Bida, G.; Barrio, J. R. *Appl. Radiat. Isot.* **1992**, *43*, 989.
(34) Bergman, R.; Solin, O. *Nucl. Med. Biol.* **1997**, *24*, 677.
(35) Coenen, H. H.; Klatte, B.; Knöchel, A.; Schüller, M.; Stöcklin, G. J. *Labelled Compd. Radiopharm.* **1986**, *23*, 455.
(36) Hamacher, K.; Coenen, H. H.; Stöcklin, G. J. *Nucl. Med.* **1986**, *27*, 235.
(37) Kim, D. W.; Ahn, D. S.; Oh, Y. H.; Lee, S.; Kil, H. S.; Oh, S. J.; Lee, S. J.; Kim, J. S.; Ryu, J. S.; Moon, D. H.; Chi, D. Y. *J. Am. Chem. Soc.* **2006**, *128*, 16394.
(38) Kim, H. J.; Jeong, J. M.; Lee, Y. S.; Chi, D. Y.; Chung, K. H.; Lee, D. S.; Chung, J. K.; Lee, M. C. *Appl. Radiat. Isot.* **2004**, *61*, 1241.
(39) Coenen, H. H. *Synthesis and Application of Isotopically Labeled Compounds*; Elsevier: Amsterdam, 1989; p 433
(40) Angeli, G.; Speranza, M.; Wolf, A. P.; Shiue, C. Y.; Fowler, J. S.; Watanabe, M. *J. Labelled Compd. Radiopharm.* **1984**, *21*, 1223.
(41) Karramkam, M.; Hinnen, F.; Berrehouma, M.; Hlavacek, C.; Vaufrey, F.; Halldin, C.; McCarron, J. A.; Pike, V. W.; Dollé, F. *Biorg. Med. Chem.* **2003**, *11*, 2769.
(42) Sandell, J.; Halldin, C.; Pike, V. W.; Chou, Y. H.; Varnas, K.; Hall, H.; Marchais, S.; Nowicki, B.; Wikström, H. V.; Swahn, C. G.; Farde, L. *Nucl. Med. Biol.* **2001**, *28*, 177.
(43) Koren, A. O.; Horti, A. G.; Mukhin, A. G.; Gündisch, D.; Dannals, R. F.; London, E. D. *J. Labelled Compd. Radiopharm.* **2000**, *43*, 413.
(44) Dollé, F. *Curr. Pharm. Des.* **2005**, *11*, 3221.
(45) Pike, V. W.; Aigbirhio, F. I. *J. Chem. Soc., Chem. Commun.* **1995**, *21*, 2215.
(46) Ross, T.; Emert, J.; Hocke, C.; Coenen, H. H. *J. Am. Chem. Soc.* **2007**, *129*, 8018.
(47) Wuest, F.; Carlson, K. E.; Katzenellenbogen, J. A. *Steroids* **2003**, *68*, 177.
(48) Chakraborty, P. K.; Kilbourn, M. R. *Appl. Radiat. Isot.* **1991**, *42*, 1209.
(49) Gulke, S.; Coenen, H. H.; Stöcklin, G. *Appl. Radiat. Isot.* **1994**, *45*, 715.
(50) Lang, L.; Eckelman, W. C. *Appl. Radiat. Isot.* **1994**, *45*, 1155.
(51) Jacobson, K. A.; Furlano, D. C.; Kirk, K. L. *J. Fluor. Chem.* **1988**, *39*, 339.
(52) Vaidyanathan, G.; Zalutsky, M. R. *Bioconjugate Chem.* **1994**, *5*, 352.
(53) Hostetler, E. D.; Edwards, W. B.; Anderson, C. J.; Welch, M. J. *J. Labelled Compd. Radiopharm.* **1999**, *42*, S720.
(54) Poethko, T.; Schottelius, M.; Thumshirn, G.; Hersel, U.; Herz, M.; Henriksen, G.; Kessler, H.; Schwaiger, M.; Wester, H. J. *J. Nucl. Med.* **2004**, *45*, 892.
(55) Kilbourn, M. R.; Dence, C. S.; Welch, M. J.; Mathias, C. J. *J. Nucl. Med.* **1987**, *28*, 462.
(56) Dolle, F.; Hinnen, F.; Vaufrey, F.; Tavitian, B.; Crouzel, C. *J. Labelled Compd. Radiopharm.* **1997**, *39*, 319.
(57) Shai, Y.; Kirk, K. L.; Channing, M. A.; Dunn, B. B.; Lesniak, M. A.; Eastman, R. C.; Finn, R. D.; Roth, J.; Jacobson, K. A. *Biochemistry* **1989**, *28*, 4801.
(58) Block, D.; Coenen, H. H.; Stöcklin, G. *J. Labelled Compd. Radiopharm.* **1988**, *25*, 201.
(59) Glaser, M.; Karlsen, H.; Solbakken, M.; Arukwe, J.; Brady, F.; Luthra, S. K.; Cuthbertson, A. *Bioconjugate Chem.* **2004**, *15*, 1447.
(60) Okarvi, S. M. *Eur. J. Nucl. Med.* **2001**, *28*, 929.
(61) Wester, H. J.; Hamacher, K.; Stöcklin, G. *Nucl. Med. Biol.* **1996**, *23*, 365.
(62) Hoehne, A.; Mu, L.; Schubiger, P. A.; Ametamey, S: M.; Graham, K.; Cyr, J. E.; Dinkelborg, L.; Stellfeld, T.; Srinivasan, A.; Voigtmann, U.; Klar, U. *J. Labelled Compd. Radiopharm.* **2007**, *50*, S6.
(63) Becaud, J.; Karramkam, M.; Mu, L.; Schubiger, P. A.; Ametamey, S: M.; Smits, R.; Koksch, B.; Graham, K.; Cyr, J. E.; Dinkelborg, L.; Suelzle, D.; Stellfeld, T.; Brumby, T.; Lehmann, L.; Srinivasan, A. *J. Labelled Compd. Radiopharm.* **2007**, *50*, S215.
(64) Ting, R.; Adam, M. J.; Ruth, T. J.; Perrin, D. M. *J. Am. Chem. Soc.* **2005**, *127*, 13094.
(65) Deng, H.; Cobb, S. L.; Gee, A. D.; Lockhart, A.; Matarello, L.; McGlinchey, R. P.; O'Hagan, D.; Onega, M. *Chem. Commun.* **2006**, *6*, 652.
(66) Schubiger, P. A.; Lehmann, L.; Friebe, M. *PET Chemistry the Driving Force in Molecular Imaging*; Springer: Berlin, 2007; p 15.
(67) Marik, J.; Sutcliffe, J. L. *Tetrahedron Lett.* **2006**, *47*, 6681.
(68) Eckelman, W. C.; Kilbourn, M. R.; Mathis, C. A. *Nucl. Med. Biol.* **2006**, *33*, 449.
(69) Sorenson, J. A.; M, R.; Phelps, M. E. *Physics in Nuclear Medicine*; Grune & Stratton: Orlando, 1987..
(70) Partridge, W. M. *Peptide Drug Delivery to the Brain*; Raven Press: New York, 2001; p 1.
(71) Clark, D. E. *Annu. Rep. Med. Chem.* **2005**, *40*, 403.
(72) Tarasaki, T.; Ohtsuki, S.; Hori, S.; Takanaga, S.; Nakashima, E.; Hosoya, K. *Drug Discovery Today* **2003**, *8*, 944.
(73) Abott, N. J. *Drug Discovery Today: Technol.* **2004**, *1*, 407.
(74) Shiue, C. Y.; Shiue, G. G.; Cornisch, K. G.; O'Rourke, M. F. *Nucl. Med. Biol.* **1995**, *22*, 613.
(75) Jaber, M.; Robinson, S. W.; Missale, C.; Caron, M. G. *Neuropharmacology* **1996**, *35*, 1503.
(76) Seeman, P.; Van Tol, H. H. M. *Trends Pharmacol. Sci.* **1994**, *15*, 264.
(77) Hall, H.; Sedvall, G.; Magnusson, O.; Kopp, J.; Halldin, C.; Farde, L. *Neuropsychopharmacology* **1994**, *11*, 245.
(78) Wagner, H. N.; Burns, H. D.; Dannals, R. F.; Wong, D. F.; Långström, B.; Duelfer, T.; Frost, J. J.; Ravert, H. T.; Links, J. M.; Rosenbloom, S. B.; Lukas, S. E.; Kramer, A. V.; Kuhar, M. *Ann. Neurol.* **1984**, *15*, S79.
(79) Farde, L.; Hall, H.; Ehrin, E.; Sedvall, G. *Science* **1986**, *231*, 258.
(80) Dewey, S. L.; Smith, G. S.; Logan, J.; Brodie, J. D.; Fowler, J. S.; Wolf, A. P. *Synapse* **1993**, *13*, 350.
(81) Breier, A.; Su, T. P.; Saunders, R.; Carson, R. E.; Kolachana, B. S.; De Bartolomeis, A.; Weinberger, D. R.; Weisenfeld, N.; Malhorta, A. K.; Eckelman, W. C.; Pickar, D. *Proc. Natl. Acad. Sci. U.S.A.* **1997**, *94*, 2569.
(82) Nyberg, S.; Nilsson, U.; Okubo, Y.; Halldin, C.; Farde, L. *Int. Clin. Psychopharmacol.* **1998**, *13*, 15.
(83) Talbot, P. S.; Laruelle, M. *Neuropsychopharmacology* **2002**, *12*, 503.
(84) Mukherjee, J.; Yang, Z. Y.; Brown, T.; Lew, R.; Wernick, M.; Ouyang, X.; Yasillo, N.; Chen, C. T.; Mintzer, R.; Cooper, M. *Nucl. Med. Biol.* **1999**, *26*, 519.
(85) Olsson, H.; Halldin, C.; Swahn, C. G.; Farde, L. *J. Cereb. Blood Flow Metab.* **1999**, *19*, 1164.
(86) Farde, L.; Halldin, C.; Stone-Elander, S.; Sedvall, G. *Psychopharmacology* **1987**, *92*, 278.
(87) Halldin, C.; Foged, C.; Chou, Y. H.; Karlsson, P.; Swahn, C. G.; Sandell, J.; Sedvall, G.; Farde, L. *J. Nucl. Med.* **1998**, *39*, 2061.
(88) Halldin, C.; Guilloteau, D.; Okubo, Y.; Lundkvist, Karlsson, P.; Chalon, S. *J. Nucl. Med.* **1998**, *39*, 118.
(89) Laakso, A.; Bergmann, J.; Haaparanta, M.; Vilkman, H.; Solin, O.; Hietala, J. *Synapse* **1998**, *28*, 244.
(90) Goodman, M. M.; Kilts, C. D.; Keil, R.; Shi, B.; Matarello, L.; Xing, D.; Votaw, J.; Ely, T. D.; Lambert, P.; Owens, M. J.; Camp, V. M.; Malveaux, E.; Hoffman, J. M. *Nucl. Med. Biol* **2000**, *27*, 1.
(91) Garnett, E. S.; Firnau, G.; Nahmias, G. *Nature* **1983**, *305*, 137.
(92) Piccini, P. *Curr. Opin. Neurol.* **2004**, *17*, 459.
(93) Nahmias, C.; Wahl, L.; Chirakal, R.; Firnau, G.; Garnett, S. *Mov. Disord.* **1995**, *10*, 298.
(94) Fowler, J. S.; MacGregor, R. R.; Wolf, A. P.; Arnett, C. D.; Dewey, S. L.; Schlyer, D.; Christman, D.; Logan, J.; Smith, M.; Sachs, H.; Aquilonius, S. M.; Bjurling, P; Halldin, C.; Hartvig, P.; Leenders, K. L.; Lundqvist, H.; Oreland, L.; Stålnacke, C. G.; Långström, B. *Science* **1987**, *235*, 481.
(95) Fowler, J. S.; Volkow, N. D.; Wang, G.-J.; Ding, Y. S.; Lewey, S. L. *Proc. Natl. Acad. Sci. U.S.A.* **1996**, *93*, 14065.
(96) Fowler, J. S.; Volkow, N. D.; Wang, G.-J.; Pappas, N.; Logan, J.; MacGregor, R.; Alexoff, D.; Shea, C.; Schyler, D.; Wolf, A. P.; Warner, D.; Zezulkova, I.; Cilento, R. *Nature* **1996**, *379*, 733.

(97) Morens, D. M.; Grandinetti, A.; Reed, D.; White, L. R.; Ross, G. W. *Neurology* **1995**, *45*, 1041.
(98) Farde, L.; Ito, H.; Swahn, C. G.; Pike, V. W.; Halldin, C *J. Nucl. Med.* **1998**, *39*, 1965.
(99) Rabiner, E. A.; Bhagwagar, Z.; Gunn, R. N.; Sargent, P. A.; Bench, C. J.; Cowen, P. J.; Grasby, P. M. *Am. J. Psychiatry* **2001**, *158*, 2080.
(100) Drevets, W. C.; Frank, E.; Price, J. C.; Kupfer, D. J.; Greer, P. J.; Mathis, C. *Nucl. Med. Biol.* **2000**, *27*, 499.
(101) Passchier, J.; van Waarde, A.; Pieterman, R. M.; Elsinga, P. H.; Pruim, J.; Hendrikse, H. N.; Willemsen, A. T. M.; Vaalburg, W. *Nucl. Med. Biol.* **2000**, *27*, 473.
(102) Carson, R. E.; Lang, L.; Watabe, H.; Der, M. G.; Adams, H. R.; Jagoda, E.; Herscovitch, P.; Eckelman, W. C. *Nucl. Med. Biol.* **2000**, *27*, 493.
(103) Sandell, J.; Halldin, C.; Chou, Y.-H.; Swahn, C.-G.; Thorberg, S.-O.; Farde, L. *Nucl. Med. Biol.* **2002**, *29*, 39.
(104) Ito, H.; Nyberg, S.; Halldin, C.; Lundkvist, C.; Farde, L. *J. Nucl. Med.* **1998**, *39*, 208.
(105) Biver, F.; Wikler, D.; Lostra, F.; Damhaut, P.; Goldman, S.; Mendlewicz, J. *Br. J. Psychiatry* **1997**, *171*, 444.
(106) Blin, J.; Sette, G.; Fiorelli, M.; Bietry, O.; Elghozi, J. L.; Crouzel, C.; Baron, J. C. *J. Neurochem.* **1990**, *54*, 1744.
(107) Szabo, Z.; Kao, P. F.; Mattews, W. B.; Ravert, H. T.; Musachio, J. L.; Scheffel, U.; Dannals, F. *Behav. Brain Res.* **1996**, *73*, 221.
(108) Ichimiya, T.; Suhara, T.; Sudo, Y.; Okubo, Y.; Nakayama, K.; Nankai, M.; Inoue, M.; Yasuno, F.; Takano, A.; Maeda, J.; Shibuya, H. *Biol. Psychiatry* **2002**, *51*, 715.
(109) Houle, S.; Ginovart, N.; Hussey, D.; Meyer, J. H.; Wilson, A. A. *Eur. J. Nucl. Med. Mol. Imaging* **2000**, *27*, 1719.
(110) Lundberg, J.; Odano, I.; Olsson, H.; Halldin, C.; Farde, L. *J. Nucl. Med.* **2005**, *46*, 1505.
(111) Jarkas, N.; Votaw, J. R.; Voll, R. J.; Williams, L.; Camp, V. M.; Owens, M. J.; Purselle, D. C.; Bremmer, J. D.; Kilts, C. D.; Nemeroff, C. B. *Nucl. Med. Biol.* **2005**, *32*, 211.
(112) Mulholland, G. K.; Kilbourn, M. R.; Sherman, P. S.; Carey, J. E.; Frey, K. A.; Koeppe, R. A. *Nucl. Med. Biol.* **1995**, *22*, 13.
(113) Zubieta, J.-K.; Koeppe, R. A.; Frey, K. A.; Kilbourn, M. R.; Magner, T. J.; Foster, N. L.; Kuhl, D. E. *Synapse* **2001**, *39*, 275.
(114) Takahashi, K.; Murakami, M.; Miura, S.; Iida, H.; Kanno, I.; Uemura, K. *Appl. Radiat. Isot.* **1999**, *50*, 521.
(115) Tsukada, H.; Takahashi, K.; Miura, S.; Nishiyama, D.; Kakiuchi, T.; Ohba, H.; Sato, K.; Hatazawa, J.; Okudera, T. *Synapse* **2001**, *39*, 182.
(116) Dewey, S. L.; MacGregor, R. R.; Brodie, J. D.; Bendriem, B.; King, P. T.; Volkow, N. D.; Schlyer, D. J.; Fowler, J. S.; Wolf, A. P.; Gatley, S. J.; Hitzemann, R. *Synapse* **1990**, *5*, 213.
(117) Nyback, H.; Halldin, C.; Ahlin, A.; Curvall, M.; Erikson, L. *Psychopharmacology* **1994**, *115*, 31.
(118) Muzic, R. F.; Berridge, M. S.; Friedland, R. P.; Zhu, N.; Nelson, A. D. *J. Nucl. Med.* **1998**, *39*, 2048.
(119) Koren, A. O.; Horti, A. G.; Mukhin, A. G.; Gündisch, D.; Kimes, A. S.; Dannals, R. F.; London, E. D. *J. Med. Chem.* **1998**, *41*, 3690.
(120) Gallezot, J. D.; Bottlaender, M.; Gregoire, M. C.; Roumenov, D.; Deverre, J. R.; Coulon, C.; Ottaviani, M.; Dollè, F.; Syrota, A.; Valette, H. *J. Nucl. Med.* **2005**, *46*, 240.
(121) Horti, A. G.; Chefer, S. I.; Mukhin, A. G.; Koren, A. O.; Gündisch, D.; Links, J. M.; Kurian, V.; Dannals, F.; London, E. D. *Life Sci.* **2000**, *7*, 463.
(122) Ding, Y. S.; Fowler, J. S.; Logan, J.; Wang, J. T.; Telang, F.; Garza, V.; Biegon, A.; Pareto, D.; Rooney, W.; Shea, C.; Alexoff, D.; Volkow, N. D.; Vocci, F. *Synapse* **2004**, *53*, 184.
(123) Kendziorra, K.; Meyer, P.; Wolf, H.; Barthel, H.; Hesse, S.; Seese, A.; Sorge, D.; Patt, M.; Becker, G.; Schildan, A.; Gertz, H. H.; Sabri, O. *Neuroimage* **2006**, *31*, T39.
(124) Meyer, P.; Hesse, S.; Kendziorra, K.; Becker, G.; Wegner, F.; Schildan, F.; Seese, A.; Lobsien, D.; Bathel, H.; Schwarz, J.; Sabri, O. *Neuroimage* **2006**, *31*, T157.
(125) Iyo, M.; Namba, H.; Fukushi, K.; Shinotoh, H.; Ngatsuka, S.; Suhara, T.; Sudo, Y.; Suzuki, K.; Irie, T. *Lancet* **1997**, *349*, 1805.
(126) Xia, W.; Ray, W. J.; Ostazewski, B. L.; Rahmati, T.; Kimberly, W. T.; Wolfe, M. S.; Zhang, J.; Goate, A. M.; Selkoe, D. J. *Proc. Natl. Acad. Sci. U.S.A.* **2000**, *97*, 9299.
(127) Shogi-Jadid, K.; Small, G. W.; Agdeppa, E. D.; Kepe, V.; Ercoli, L. M.; Siddarth, P.; Read, S.; Satyamurthy, N.; Petric, A.; Huang, S.-C.; Barrio, J. R. *Am. J. Geriatr. Psychiatry* **2002**, *10*, 24.
(128) Rowe, C. C.; Ng, S.; Ackermann, U.; Gong, S. J.; Pike, K.; Savage, G.; Cowie, T. F.; Dickinson, K. L.; Maruff, P.; Darby, B.; Smith, C.; Woodward, M.; Merory, J.; Tochon-Danguy, H.; O'Keefe, G.; Klunk, W. E.; Mathis, C. A.; Price, J. C.; Masters, C. L.; Villemagne, V. L. *Neurology* **2007**, *68*, 1718.
(129) Verhoeff, N. P.; Wilson, A. A.; Takeshita, S.; Trop, L.; Hussey, D.; Singh, K.; Kung, H. F.; Kung, M. P.; Houle, S. *Am. J. Geriatr. Psychiatry* **2004**, *12*, 584.
(130) Rowe, C.; Ng, S.; Ackermann, U.; Brown, W.; O'Keefe, G.; Tochon-Danguy, H.; Chan, G.; Kung, H. F.; Kung, M. P.; Skovronsky, D.; Dyrks, T.; Holl, G.; Krause, S.; Friebe, M.; Lehmann, L.; Lindermann, S.; Sittner, W.; Dinkelborg, L.; Masters, C.; Villemagne, V. L. *J. Nucl. Med. Meeting Abstracts* **2007**, *48*, 57.
(131) Meador-Wooddruff, J. H.; Healy, D. J. *Brain Res. Rev.* **2002**, *32*, 288.
(132) Tatarczynska, E.; Klodinska, E.; Chojnacka-Wojcik, E.; Parucha, A.; Gasparini, F.; Kuhn, R.; Pilc, A. *Br. J. Pharmacol.* **2001**, *132*, 1432.
(133) Spooren, W. P.; Vassout, A.; Neijt, H. C.; Kuhn, R.; Gasparini, F.; Roux, S.; Posolt, R. D.; Gentsch, C. *J. Pharmacol. Exp. Ther.* **2000**, *295*, 1267.
(134) Ohnuma, T.; Augood, S. J.; Arai, H.; McKenna, P. J.; Emson, P. C. *Brain Res. Mol. Brain Res.* **1998**, *56*, 207.
(135) Rouse, S. T.; Marino, M. J.; Bradley, S. R.; Awad, H.; Wittmann, M.; Conn, P. J. *Pharmacol. Ther.* **2000**, *88*, 427.
(136) Chiamulera, C.; Epping-Jordan, M. P.; Zocci, A.; Marcon, C.; Cottiny, C.; Tacconi, S.; Corsi, M.; Orzi, F.; Conquethave, F. *Nat. Neurosci.* **2001**, *4*, 873.
(137) Sotgiu, M. E.; Bellomi, P.; Biella, G. E. *Neurosci. Lett.* **2003**, *342*, 85.
(138) Walker, K.; Reeve, A.; Bowes, M.; Passena, M.; Davis, A.; Gentry, A.; Kesingland, A.; Gasparini, F.; Spooren, W; Stoehr, N.; Pagano, A.; Flor, P. J.; Vranesic, I.; Lingenhoehl, K.; Johnson, E. C.; Varney, M.; Urban, L; Kuhn, R. *Neuropharmacology* **2001**, *40*, 10.
(139) Blin, J.; Denis, A.; Yamaguchi, T.; Crouzel, C.; MacKenzie, E. T.; Baron, J. C. *Neurosci. Lett.* **1991**, *121*, 183.
(140) Ametamey, S. M.; Kneifel, S.; Brühlmeier, M.; Kokic, M.; Honer, M.; Arigoni, M.; Buck, A.; Samnick, S.; Quack, G.; Schubiger, P. A. *Nucl. Med. Biol.* **2002**, *29*, 227.
(141) Hartvig, P.; Valtysson, J.; Lindner, K. J.; Kristensen, J.; Karlsten, R.; Gustafsson, L. L.; Persson, J.; Svensson, J. O.; Oye, I.; Antoni, G. *Clin. Pharmacol. Ther.* **1995**, *58*, 165.
(142) Hamill, T. G.; Krause, S.; Ryan, C.; Bonnefous, C.; Govek, C.; Seiders, T. J.; Cosford, N. D. P.; Roppe, J.; Kamenecka, T.; Patel, S.; Gibson, R. E.; Sanabria, S.; Riffel, K.; Eng, W.; King, C.; Yang, X.; Green, M. D.; O'Malley, S. S.; Hargreaves, R.; Burns, H. D. *Synapse* **2005**, *56*, 205.
(143) Siméon, F. G.; Brown, A. K.; Zoghbi, S. M.; Patterson, V. M.; Innis, R. B.; Pike, V. W. *J. Med. Chem.* **2007**, *50*, 3256.
(144) Ametamey, S. M.; Kessler, L. J.; Honer, M.; Wyss, M. T.; Buck, A.; Hinterman, S.; Auberson, Y. P.; Gasparini, F.; Schubiger, P. A. *J. Nucl. Med.* **2006**, *47*, 698.
(145) Ametamey, S. M.; Treyer, V.; Streffer, J.; Wyss, M. T.; Schmidt, M.; Blagoev, M.; Hintermann, S.; Auberson, Y.; Gasparini, F.; Fischer, U. C.; Buck, A. *J. Nucl. Med.* **2007**, *48*, 247.
(146) Chatziioannou, A. F. *Eur. J. Nucl. Med.* **2002**, *29*, 98.
(147) Hume, S. P.; Jones, T. *Nucl. Med. Biol.* **1998**, *25*, 729.
(148) Honer, M.; Hengerer, B.; Blagoev, M.; Hintermann, S.; Waldmeier, P.; Schubiger, P. A.; Ametamey, S. M. *Nucl. Med. Biol.* **2006**, *33*, 607.
(149) Opacka Juffry, J.; Ahier, R. G.; Cremer, J. E. *Synapse* **1991**, *7*, 169.
(150) Tsukada, H.; Nishiyama, S.; Kakiuchi, T.; Ohba, H.; Sato, K.; Harada, N.; Nakanishi, S. *Brain Res.* **1999**, *849*, 85.
(151) Votaw, J. R.; Byas-Smith, M. G.; Voll, R.; Halkar, R.; Goodman, M. M. *Anesthesiology* **2004**, *101*, 1128.
(152) Honer, M.; Bruhlmeier, M.; Missimer, J.; Schubiger, P. A.; Ametamey, S. M. *J. Nucl. Med.* **2004**, *45*, 464.
(153) Matsumura, A.; Mizokawa, S.; Tanaka, M.; Wada, Y.; Nozaki, S.; Nakamura, F.; Shiomi, S.; Ochi, H.; Watanabe, Y. *NeuroImage* **2003**, *20*, 2040.
(154) Tsukada, H.; Sato, K.; Kakiuchi, T.; Nishiyama, S. *Brain Res.* **2000**, *857*, 158.
(155) Noda, A.; Takamatsu, H.; Minoshima, S.; Tsukada, H.; Nishimura, S. *J. Cereb. Blood Flow Metab.* **2003**, *23*, 1441.
(156) Hassoun, W.; Le Cavorsin, M.; Ginovart, N.; Zimmer, L.; Gualda, V.; Bonnefoi, F.; Leviel, V. *Eur. J. Nucl. Med.* **2003**, *30*, 141.
(157) Zimmer, L.; Fournet, G.; Benoit, J.; Guillaumet, G.; Le Bars, D. *Nucl. Med. Biol.* **2003**, *30*, 541.
(158) Momosaki, S.; Hatano, K.; Kawasumi, Y.; Kato, T.; Hosoi, R.; Kobayashi, K.; Inoue, O.; Ito, K. *Synapse* **2004**, *54*, 207.
(159) Vaska, P.; Woody, C. L.; Schlyer, D. J.; Shokouhi, S.; Stoll, S. P.; Pratte, J.-F.; O'Connor, P.; Junnarkar, S. S.; Rescia, S.; Yu, B.; Purschke, M.; Kandasamy, A.; Villanueva, A.; Kriplani, A.; Radeka, V.; Volkow, N.; Lecomte, R.; Fontaine, R. *IEEE Trans. Nucl. Sci.* **2004**, *51*, 2718.
(160) LaForest, R.; Sharp, T. L.; Engelbach, J. A.; Fettig, N. M.; Herrero, P.; Kim, J.; Lewis, J. S.; Rowland, D. J.; Tai, Y. C.; Welch, M. J. *Nucl. Med. Biol.* **2005**, *32*, 679.
(161) Rubins, D. J.; Meadors, A. K.; Yee, S.; Melega, W. P.; Cherry, S. R. *J. Neurosci. Methods* **2001**, *107*, 63.
(162) Hume, S. P.; Lammertsma, A.; Myers, R.; Rajeswaran, S.; Bloomfield, P. M.; Ashworth, S.; Fricker, R. A.; Torres, E. M.; Watson, I.; Jones, T. *J. Neurosci. Methods* **1996**, *67*, 103.

CR0782426